BUKTI KORESPONDENSI
ARTIKEL JURNAL INTERNASIONAL BEREPUTASI

Judul artikel : Analysis of an Axial Permanent Magnetic Bearing for 1MW Horizontal Axis Wind Turbine
Jurnal : Journal of Advanced Research in Fluid Mechanics and Thermal Sciences
Penulis : Kriswanto, S.Pd., M.T.

No.	Perihal	Tanggal
1.	Bukti konfirmasi submit artikel dan artikel yang disbumit	10 Oktober 2021
2.	Bukti konfirmasi review dan hasil review pertama	27 Oktober 2021
3.	Bukti konfirmasi submit revisi, respon kepada reviewer, dan artikel yang diresubmit	13 November 2021
4.	Bukti konfirmasi artikel *accepted submission*	14 November 2021
5.	Bukti konfirmasi artikel *production* (*copyedited*)	25 April 2022
6.	Bukti Konfirmasi publish	24 Mei 20022
7.	Bukti Konfirmasi available in SCOPUS	14 Juni 2022
8.	Artikel available online	11 April 2022

1. Bukti konfirmasi submit artikel dan artikel yang disubmit (10 Oktober 2021)

UNNES
UNIVERSITAS NEGERI SEMARANG

Kriswanto Unnes <kriswanto@mail.unnes.ac.id>

[J. Adv. Res. Fluid Mech. Therm. Sc.] Submission Acknowledgement

Dr. Nor Azwadi Che Sidik <azwadi@semarakilmu.com.my>   Sun, Oct 10, 2021 at 6:02 PM
To: Kriswanto <kriswanto@mail.unnes.ac.id>

Kriswanto:

Thank you for submitting the manuscript, "EIC-Analysis of an Axial Permanent Magnetic Bearing for 1MW Horizontal Axis Wind Turbine " to Journal of Advanced Research in Fluid Mechanics and Thermal Sciences. With the online journal management system that we are using, you will be able to track its progress through the editorial process by logging in to the journal web site:

Submission URL: https://semarakilmu.com.my/journals/index.php/fluid_mechanics_thermal_sciences/authorDashboard/submission/9

[Quoted text hidden]

Journal of Advanced Research in Fluid Mechanics and Thermal Sciences

🔔 👤

← Back to Submissions

9 / **Kriswanto et al.** / Analysis of an Axial Permanent Magnetic Bearing for 1MW Horizor   **Library**

Workflow	**Publication**

Submission	**Review**	**Copyediting**	**Production**

Submission Files

🔍 **Search**

▶ 📄 | 10 | **B007.docx**   October 10, 2021   Article Text

Download All Files

Pre-Review Discussions

Add discussion

Name	From	Last Reply	Replies	Closed
		No Items		

Analysis of an Axial Permanent Magnetic Bearing for 1MW Horizontal Axis Wind Turbine

Kriswanto[1], R F Naryanto[1,] R Prasdiansyah[1], D H Al-Janan[1], S Anis[1], W Sumbodo[1], W. Aryadi[1], A. Roziqin[1], and J Jamari[2]

[1]Department of Mechanical Engineering, Universitas Negeri Semarang, Gd E9 Kampus Sekaran Gunungpati, Semarang, Indonesia
[2]Department of Mechanical Engineering, University of Diponegoro, Jl. Prof. Sudharto Kampus UNDIP Tembalang, Semarang 50275, Indonesia

[1]kriswanto@mail.unnes.ac.id

Abstract. One way to reduce maintenance costs while improving wind turbine efficiency is to replace mechanical bearings with permanent magnetic bearings. The permanent magnetic bearing is a free contact bearing in which the rotor is elevated from the stator by the magnet's repelling force. The purpose of this study is to analyze the variation of permanent magnet width and the gap distance between the rotor-stator magnets that can produce the magnetic axial force opposing the thrust force of 1MW horizontal axis wind turbines (HAWT). The method used in this study is a magnetic force simulation using finite element method by varying the magnet thickness, width of the gap, and displacement between the rotor-stator of the PMB model. The PMB model consists of rotor and stator magnets arranged in 3 layers with Nd2Fe14B type material with a magnetic flux density of 1.45 T. Variations in thickness of the rotor and stator magnets are 0.1; 0.15, respectively; 0.2 (m), while variations in the width of the magnetic gap are 4, 5, 6 (mm). The results of the study found that the displacement that produces an axial magnetic force that can support a thrust force of 199.5kN is the lowest in the PMB model with a magnetic thickness of 0.15m with a magnetic gap of 4mm, while the highest is at a magnetic thickness of 0.1m with a magnet gap of 6mm. The greater the thickness of the PMB axial magnet design, the greater the displacement that provides zero axial magnetic forces. Further, the maximum of the magnetic axial force is rise on with increasing magnet thickness.

1. Introduction

One of the most critical components of wind turbines is the bearing. Furthermore, bearing failure is contributes to wind turbine generator failure in general [1]. Large-scale power plants in Indonesia currently apply mechanical bearings for onshore wind turbines with a capacity of 3.6 MW. One of the most critical components of wind turbines is the bearing. Furthermore, bearing failure is contributes to wind turbine generator failure in general [1]. Large-scale power plants currently apply mechanical bearings for onshore and offshore wind turbines. Nevertheless, the use of it has a limited service life as well as capability [2]. So the effort to improve the efficiency and reliability of wind turbines is to minimize friction using magnetic bearings [3]. The magnetic bearing is a bearing that utilizes refuse forces to support a rotor without physical contact [4].

Magnetic bearings have the benefit of being able to adapt to changing operating conditions and the environment. Within certain limits, the adjustment of magnetic bearing caused vibration was

independent of the rotor position. Moreover, magnetic bearings can maintain rotor equilibrium positions at various loads. The rotor can rotate on its main axis and does not cause vibration on the foundation. Due to the levitation force of magnets, the vibration was significantly reduced [5]. In addition, the magnetic levitation system helps the rotor rotate with minimal friction, affect the bearing lifetime becomes longer. The friction on a magnetic bearing is small except with air so that the blades can rotate easily [6]. Nevertheless, permanent magnetic bearings (PMB) have several problems, including stability problems. Otherwise, given the long lifetime of its use then PMB is an effective solution to overcome the bearing problems [7]. The study of PMB in wind turbine prototypes to substitute mechanical bearings can enhance rotational speed and torque, therefore enhancing Horizontal Axis Wind Turbine (HAWT) performance [8]. Comparative study of axial force results of PMB between analytical approach and finite element method shows good agreement between the two [9]

The permanent magnetic bearing has been applied for rotating shafts that are used to replace conventional bearings which have high maintenance costs and friction [11]. Therefore, maintenance costs of wind turbines can be minimized by the use of permanent magnetic bearings. It is aligned with the statement that passive magnetic bearing is one of the most economical and effective methods to lift the two surfaces in relative motion that do not require active control and additional energy [12].

The study of modeling of the axial permanent magnetic bearing that comparing the theoretical simulation of the Monte Carlo method and the finite element method found that errors approximate zero and are consistent. Moreover, the experimental results are consistent with the simulation analysis [13].

The previous study [3-8][10-12] shows the permanent magnetic bearings reduce friction, minimizes maintenance costs, can replace mechanical bearings. While none of the above literature has developed or studied the axial force of a PMB for a 1MW HAWT. The main shaft bearing of the HAWT must support both radial and axial loads (thrust forces). Furthermore, the HAWT thrust force is affected by the cut in and cut out of wind speed. The higher the wind speed, the higher the axial load on the main shaft bearing HAWT. Therefore, this paper presents to analyzes the axial magnetic force of the several thicknesses and air gaps of the permanent magnetic bearing models as the main bearing of the 1MW HAWT. Magnetic force and displacement are analyzed to find the shortest gap that can sustain the highest thrust force (at the cut out of wind speed). The main bearing locates near the gearbox, as shown in Figure 1 and indicated by number 2.
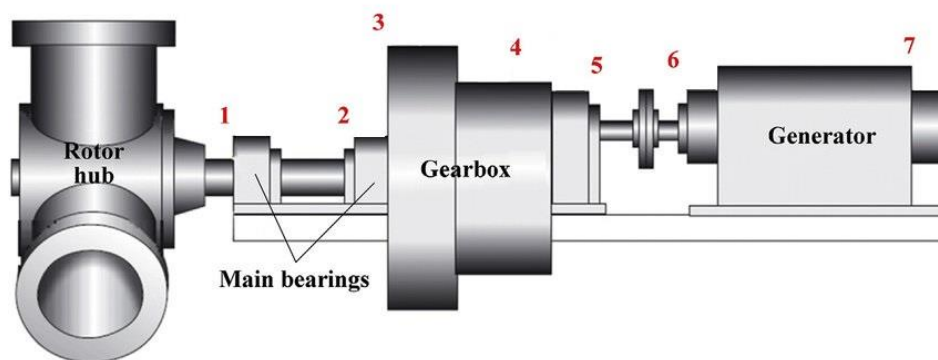

Figure 1. Main shaft bearings [10]

2. Method

The main shaft of the HAWT model, made of 34CrNiMo6 steel, complies with wind turbine certification standards [14]. Furthermore, it was analyzed by finite element method and confirmed by Mohr II theory calculations to get the deflection value due to radial load. The defection will be used as the minimum air gap to prevent collisions between the rotor magnets and the stator magnets. The material properties of 34CrNiMo6 steel used in the finite element method are the density of 7800 (kg/m^3), elasticity modulus by 210 GPa, and Poisson's ratio of 0.3 [15]. The main shaft must be safe during operation to prevent damage that causes unexpected economic losses [16]. Furthermore, the 34CrNiMo6 steel has good toughness properties also the shock resistance of the material is good enough in the operating

environment temperature [17]. In addition to being applied to wind turbine shafts, 34CrNiMo6 is high-strength structural steel frequently used in large-sized shaft components with complex geometry, such as aircraft propeller shafts and automobile connecting rods [18-19]. The specifications for the horizontal axis wind turbine show in Table 1.

Table 1. HAWT model specifications

Part name	Specification	Value
Rotor Blade	Number of blades	3
	Diameter (m)	54.4
	power coefficient, C_P	0.4877
	Tip Speed Ratio, TSR	2.82
	Rotor Load (N)	164150
Main shaft	Density, ρ (kg/m³)	7800
	Diameter (m)	1.25
	Massa, m (Kg)	404.3
	Length, l (m)	4.5
	Material	34CrNiMo6
Bearing	Diameter Bore (m)	1.25
	Outer diameter (m)	2.2
	Material	$Nd_2Fe_{14}B$
	Remanent flux density, B_r (T)	1.45
Control	Cut in speed (m/s)	3.5
	Cut out speed (m/s)	15

The maximum deflection is the distance of the shaft to prevent the possibility of friction between the stator magnet and the rotor magnet. This calculation uses two methods, namely the finite element analysis method and Mohr's Theory calculation. The bending moment diagram on the HAWT main shaft shows in Figure 2.
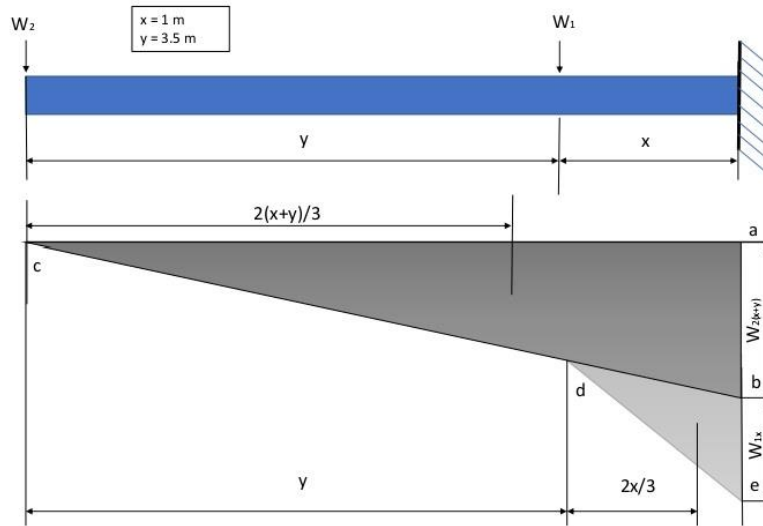

Figure 2. Bending moment diagram of HAWT main shaft

Which x (m) is the distance from the base of the shaft to the center of the magnetic load, y is the distance from the center of gravity to the end shaft (m), W_1 is the rotor magnet load (N), and W_2 is the total load from the connector hub load and the rotor load (N). Hereafter, the equations (1-2) for the deflection calculations.

$$I_P = \pi 4 (r_{c2}{}^4 - r_{c1}{}^4) \tag{1}$$

$$\delta = \frac{1}{EI} \int_X^Y M\, x\, dx \tag{2}$$

Where I_P is the polar inertia of the shaft, r_{c1} is the inner radius of the shaft cylinder, r_{c2} is the outer radius of the shaft cylinder, E modulus of elasticity of 34CrNiMo6, M is an area of the bending moment diagram, x is the distance of the load to the base of the shaft, and δ is the maximum deflection of the shaft. The data for each variable is present in Table 2.

Table 2. Properties on HAWT main shaft

x [m]	y[m]	W_1 [N]	W_2 [N]	r_{c1} [m]	r_{c2} [m]	E [GPa]
1	3.5	17,283	164,150	0.225	0.625	210

The location of the axial PMB on the HAWT main shaft is shown in Figure 3, wherein the position is closer to the gearbox. The free-body diagram of the force and moment on the main shaft see in Figure 4. The thrust force received by the rotor from the wind calculate using Equation 4.

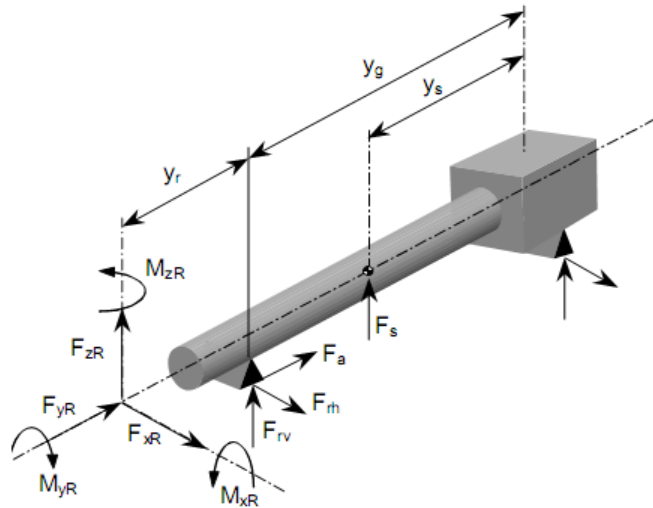**Figure 3.** Location of axial PMB on the HAWT main shaft

Figure 4. Forces and moments on the HAWT main shaft [20]

$$A = \pi\, r2 \tag{3}$$

$$F_{yR} = \frac{1}{2}\, \rho\, A\, (v_1^2 - v_2^2) \tag{4}$$

The magnetic force simulation in this study uses the finite element method assisted by COMSOL Multiphysics 5.5 by integrating vector Equations (5). The axial force of the PMB model was simulation by displacement distance between the rotor magnet against the stator.

$$f = n.T = -\frac{1}{2}n(H.B) + (n.H)B^T \tag{5}$$

Where f is the magnetic force (n), n is the external normal vector, T is the tensor stres Maxwell, H is the magnetic field/ coercivity, B is the magnetic flux density (T).

The magnetic model uses the relationship between the density of the magnetic lines force and the magnetic field, which is expressed by Equation 6.

$$B = \mu_r\mu_0 H \tag{6}$$

Where μ_r is the relative permeability and μ_0 is the absolute magnetic permeability.

Magnetic field using Ampere's law model, with the stationary magnetic field Equation 7.

$$B = \bar{V}A' \tag{7}$$

$$\mu_0^{-1}\mu_r^{-1}\overline{V}\,A' = J \tag{8}$$

Where $\bar{V}$ is the vector operators, A' is the Magnetic potential vector, and J is the magnetization residual or magnetism induction density.

Boundary conditions using the Equation 9.

$$n_1 A' = 0 \tag{9}$$

The magnetic field was the model using a magnetic field interface model. Ampere's law used to include magnetic field physics into all free air domains. The infinite element domain uses to simulate the large region of free space surrounding the magnets. The material for all free domains is air. The free triangular mesh generated in the simulation is both the computational domain and the magnets.

In this study, the magnet material made from $Nd_2Fe_{14}B$, which the magnet is composed of a mixture of neodymium (Nd), iron powder (Fe), and boron powders (B) using the high compression molding method [21]. The $Nd_2Fe_{14}B$ is a kind of hard magnet with excellent magnetic characteristics, possesses the highest values of maximum energy product (BH) max and coercivity [22-24]. In addition, $Nd_2Fe_{14}B$ is the strongest permanent magnet because maximum energy reaches more than $400kJ/m^3$ [25-27]. Figure 5 show the HAWT main shaft design, all dimensional units of mm. The diameter of the HAWT main shaft is a limitation in determining the inner diameter of the PMB rotor magnet.
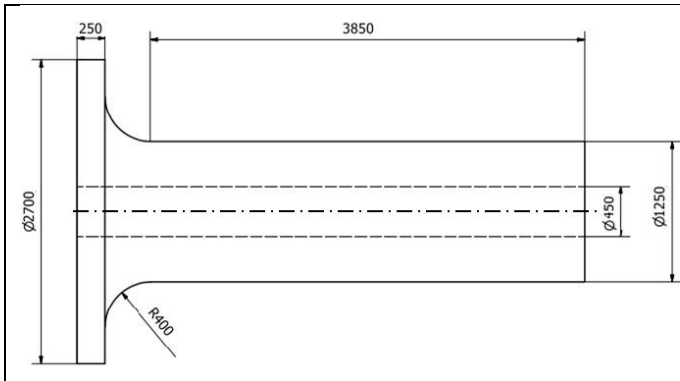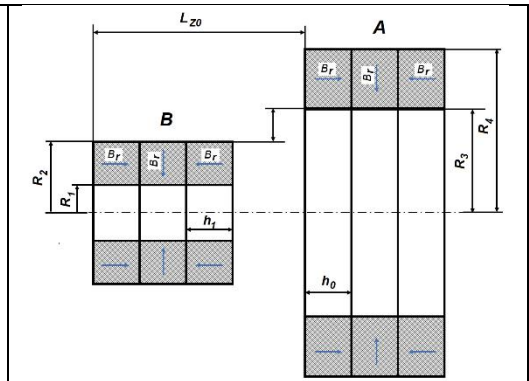

Figure 5. HAWT main shaft design	**Figure 6**. Design of axial PMB configuration

As illustrated in Figure 6, the PMB axial configuration design includes three magnets on the rotor magnet B and the stator magnet A, which has a magnetic force density direction like in Figure. The rotor magnet is an inner magnet with an outer diameter smaller than the stator magnet's inner diameter, resulting in a gap. Placement of the rotor magnet against the stator, $LZ0$ must be in a condition where there is no axial magnetic force interaction between the two ($F_z=0N$). This setting is a condition when the wind turbine rotor does not receive thrust force from the wind. Meanwhile, the maximum thrust

force or at the cut-out wind speed must restrain by the PMB thrust force with the smallest possible displacement distance (ΔZ).

The design specifications of the axial PMB model are presented in Table 3, wherein the model uses a configuration of concentric ring permanent magnets which have different dimensions and have opposite directions of magnetic force density (Br). Furthermore, the axial PMB in the present study functions as the axial main shaft bearing of HAWT.

Table 3. PMB model specifications

	Outer magnet, A	**Inner magnet, B**
Inner Radius (m)	$R_3 = 0.805; 0.806; 0.8067$	$R_1 = 0.625$
Outer Radius (m)	$R_4 = 1.1$	$R_2 = 0.8$
Thickness (m)	$h_0 = 0.1; 0.15; 0.2$	$h_1 = 0.1; 0.15; 0.2$
Magnetic Flux Density, Br (T)	1.45	1.45

3. Results and Discussion

3.1. Thrust force on the HAWT main shaft

The Thrust force (F_{yR}) of the HAWT main shaft is calculated by equation (3), which A of 2323.098 m^2 and ρ is the air density assumed is 1.293 kg/m^3. The thrust force results on the HAWT main shaft are shown in Figure 7.

The minimum thrust force is 10862.22 N generated at a wind speed of 3.5 m/s at the cut-in of HAWT, while the maximum is 199.5kN generated at a wind speed of 15 m/s, namely at a HAWT cut-out. The higher the wind speed, the higher the thrust force. According to Figure 7, the HAWT main shaft bearing must sustain an thrust force of 199.5 kN
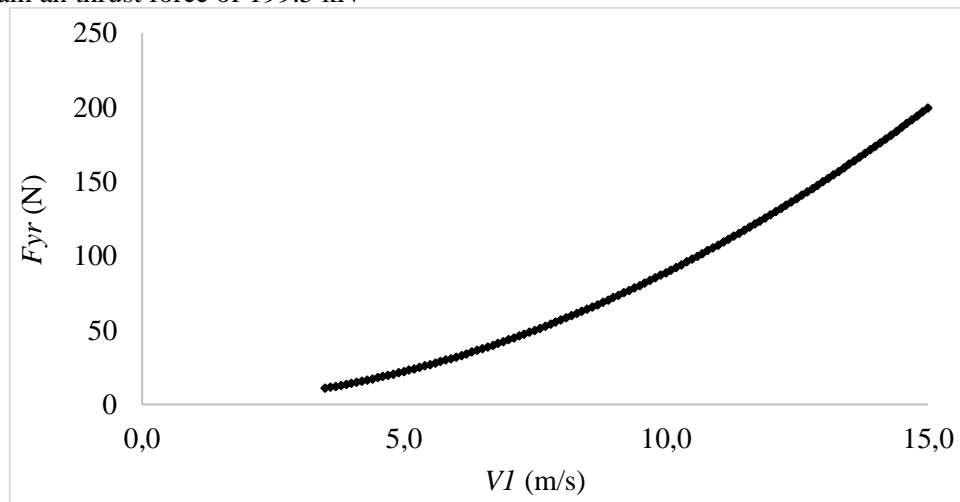

Figure 7. Graph of the thrust force on the HAWT main shaft vs windspeed

3.2. Maximum deflection on the main shaft of HAWT

The maximum deflection is analyzed to determine the minimum gap between the rotor magnets and the stator not to touch later. The results obtained from the finite element method (FEM) use COMSOL will then compare with mathematical of the Mohr II theoretical equation. The results of the maximum deflection analysis show in Figure 8.
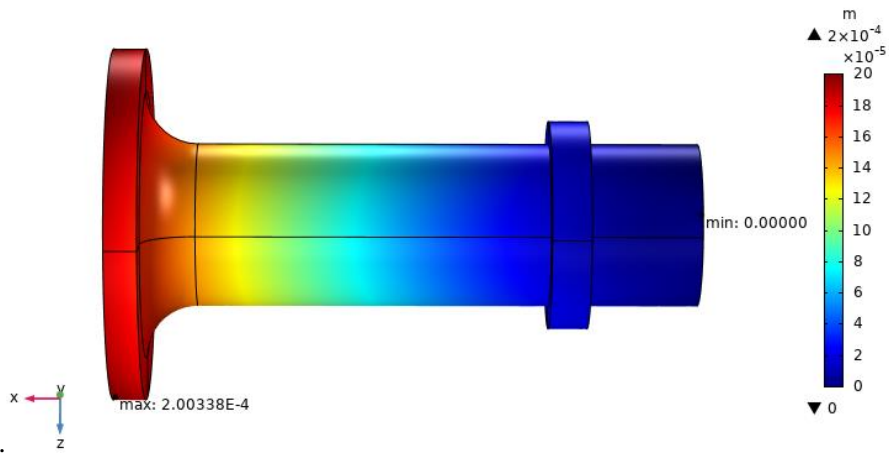
Figure 8. Maximum deflection of HAWT main shaft use FEM

Table 4. Model Validation with Mohr II theory

	FEM	Analytic	Variation (%)
Maximum Deflection (mm)	0.20033	0.20036	0,015

The maximum deflection of the modeling approximates analytic calculations using Mohr II theory (see Table 4). Moreover, the discrepancy between the two methods above has 0.015 %, which indicates that the modeling method is declared valid.

3.3. *PMB model validation*

Figure 8 is a plot of axial force versus displacement generated from the modeling, where the axial force *Fz* is 126.12 N, is the rotor magnet experiences an of the stator as far as 6mm towards the positive axial direction *dZ*. This also applies to the displacement that leads to negative axial where at *dZ* at a distance of -6mm an axial force *Fz* equal to -126.12 N is produced.
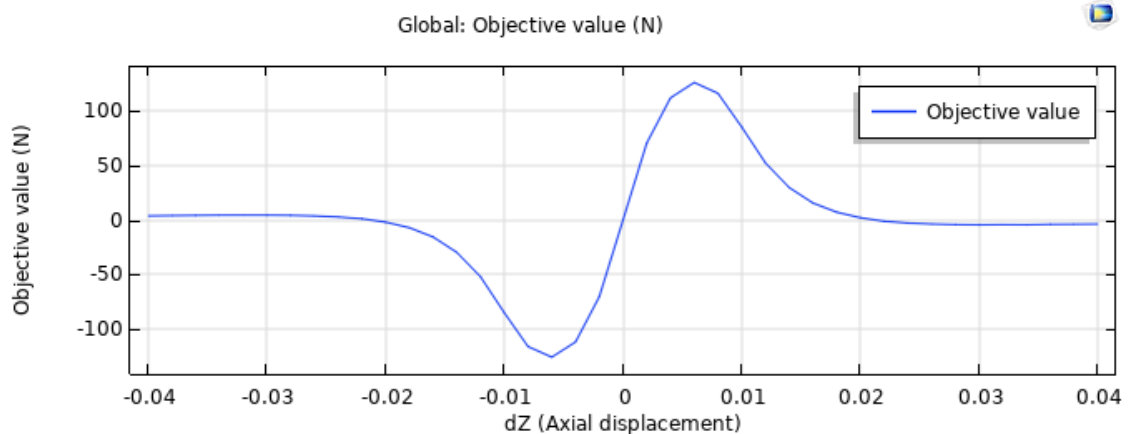

Figure 8. Plot of the magnetic axial force of the modelling

Table 5 Validation of the axial force with Bekinal model

	Modeling	Bekinal model [28]	Variation (%)
Axial Force (N)	126.12	126.59	0.37

The maximal axial force obtained through modeling is 126.12N, whereas the Bekinal mathematical model yields 126.59N (see Table 5). The discrepancy between the results of the two methods is 0.37%, which indicates that the modeling method is declared valid.

3.4. Axial force modeling of 0.1 m magnet thickness of the PMB

The axial PMB design is depicted in Figure 6, then the parameters provided in Table 1 have values of h_0-h_1 indicate a magnet thickness of 0.1 m. The variation in this configuration lies in the width of the magnetic gap with R_3 values are 0.805, 0.806, 0.807 (m), so that the magnetic gap c becomes 4 mm, 5 mm, and 6 mm. The maximum magnetic flux density of 1.45T (see Figure 9-a) at 0.1 m thickness variation and 4mm gap as shown in the red area concentrated in the center of the magnet both on the rotor and stator. Figure 9-b depicts the axial force towards displacement with dZ – 0.38 m to 0.38 m.
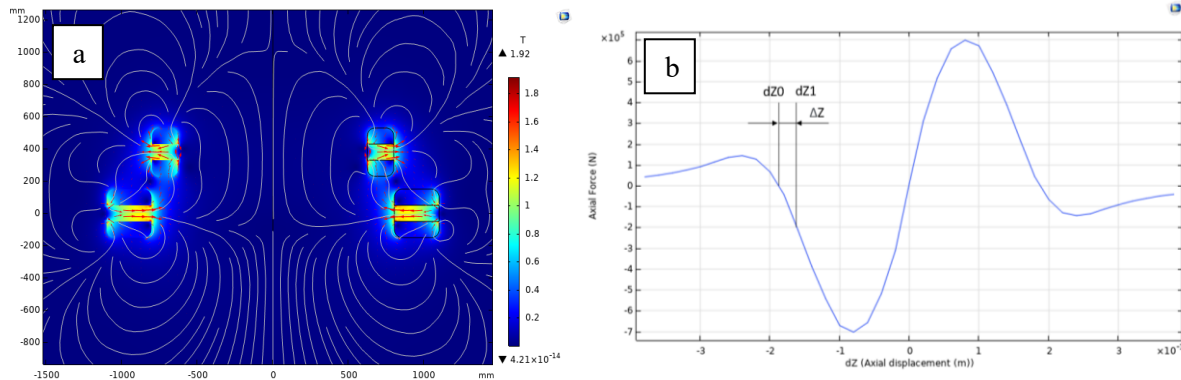

Figure 9. Plot of the axial PMB h_0 h_1 0.1 m, c 4mm, (a) magnetic flux density (b) axial force-displacement range dZ -0.38 to 0.38 m
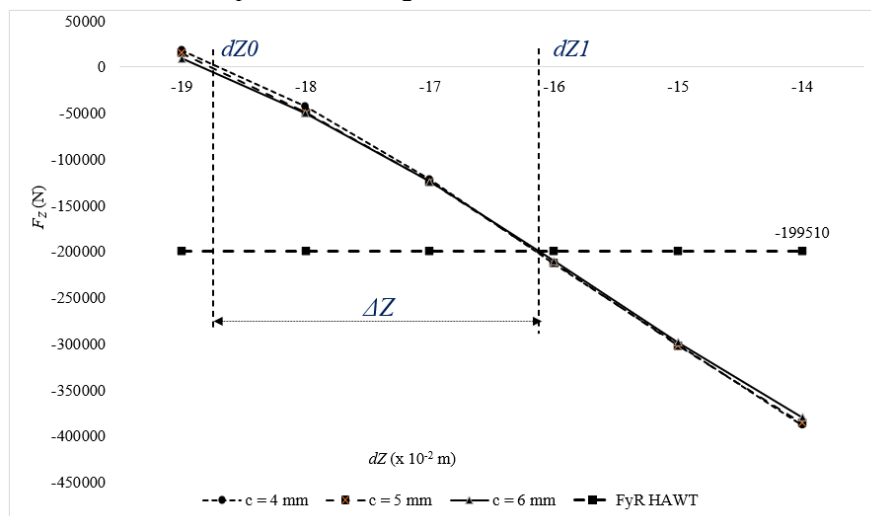

Figure 10. The plot of the axial force-displacement of axial PMB, with h 0.1 m

Figure 10 is a plot of the axial force versus displacement generated in the axial PMB simulation with a magnetic thickness of 0.1 m which the width is varied for the magnetic gap "c" (4mm; 5mm; and 6mm) and for the distance set at dZ –190mm to -140mm. The rotor-stator distance that produces 0N ($LZ0$) magnetic axial force is 187mm. The measurement of ΔZ starts from the displacement point of the rotor-stator at an axial force of 0N ($dZ0$) to the location ($dZ1$) wherein F_Z 199.5 kN is produced. The thrust force on the HAWT main shaft, which is 199.5 kN, can be supported by axial PMB at c 4mm with displacement ΔZ 26mm, c 5mm with ΔZ 27mm, and c 6mm, the distance ΔZ is 28mm. Based on the simulation results, the most optimum axial force is found at c 4mm because it has the smallest displacement (ΔZ) value among the other configuration. Furthermore, this configuration can support the axial load on the HAWT main shaft with a ΔZ value of 2.6mm.

3.5. Axial force modeling of 0.15 m magnet thickness of the PMB

The axial PMB design uses the parameters provided in Table 1 have values of *h0-h1* indicate a magnet thickness of 0.15 m. The difference in this configuration magnetic gap *c* values of 4mm, 5mm, and 6mm. Figure 11-a shows the maximum magnetic flux density of 1.45T at 0.15 m thickness variation and 4mm gap, which is centered in the magnet's center on both the rotor and stator. Figure 11-b shows the axial force-displacement which *dZ* – 0.38 m to 0.38 m.
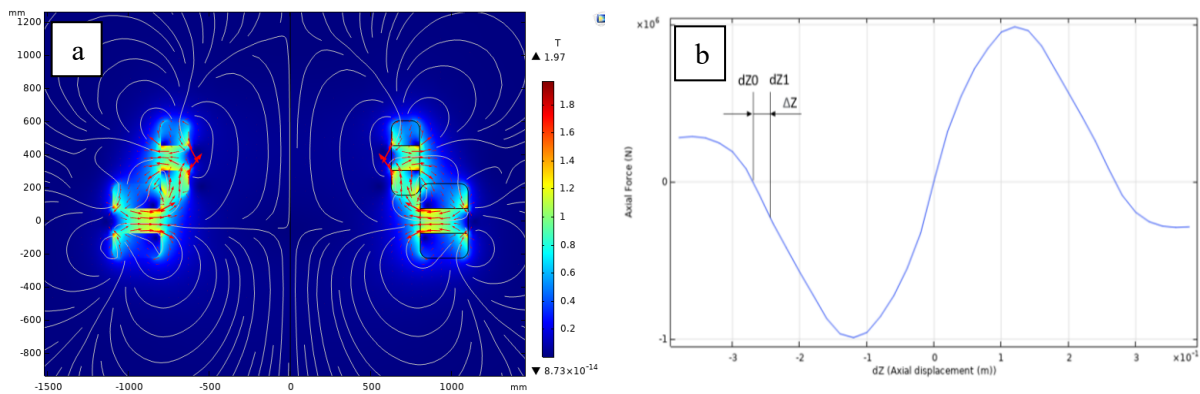

Figure 11. Plot of the axial PMB h_0 h_1 0.15 m, c 4mm, (a) magnetic flux density (b) axial force-displacement range *dZ* -0.38 to 0.38 m
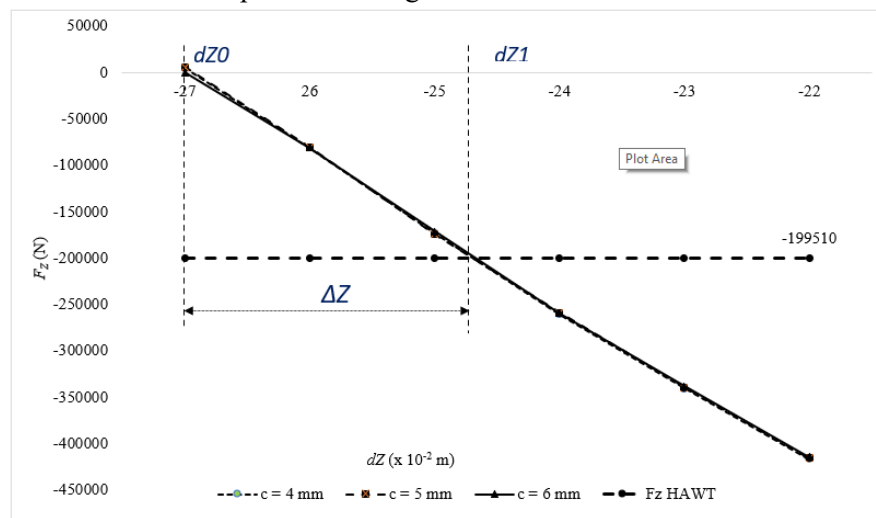

Figure 12. Plot of the axial force -displacement of axial PMB, with h 0.15 m

Figure 12 shows a plot of the axial force against displacement created in the axial PMB simulation with a magnetic thickness of 0.15 m and a magnetic gap "*c*" (4mm; 5mm; 6mm) and a distance set at *dZ* – 270mm to -220mm. The rotor-stator distance required to generate (*LZ0*) 0 N magnetic axial force is 270mm.The thrust force of 199.5 kN on the HAWT main shaft may be sustained by axial PMB at c 4mm with displacement *ΔZ* 22mm, c 5mm with displacement *ΔZ* 22mm, and *c* 6mm with distance *ΔZ* 23mm. According to the results, the most optimum axial force is discovered at *c* 4mm since it has the minimum displacement (*ΔZ*) value among the other configurations. Furthermore, with a *ΔZ* value of 22mm, this arrangement can sustain the axial load on the HAWT main shaft. The simulation results of the axial magnetic force at 0.15m thickness of the magnet is similar to 0.1m thickness configuration, wherein the air gap (*c*) the smaller the displacement smaller too.

3.6. Axial force modeling of 0.2 m magnet thickness of the PMB

The axial PMB design proposes the specifications shown in Table 1, with h_0-h_1 indicating a magnet thickness of 0.2m. The magnetic gap c values of 4mm, 5mm, and 6mm differ in this arrangement. Figure 13-a depicts the maximum magnetic flux density of 1.45T in the central magnetic region of the rotor

and stator, for 0.2 m thickness variation and 4mm gap of the axial PMB Design. Figure 13-b depicts the axial force-displacement relationship with $dZ - 0.38$ m to 0.38 m.
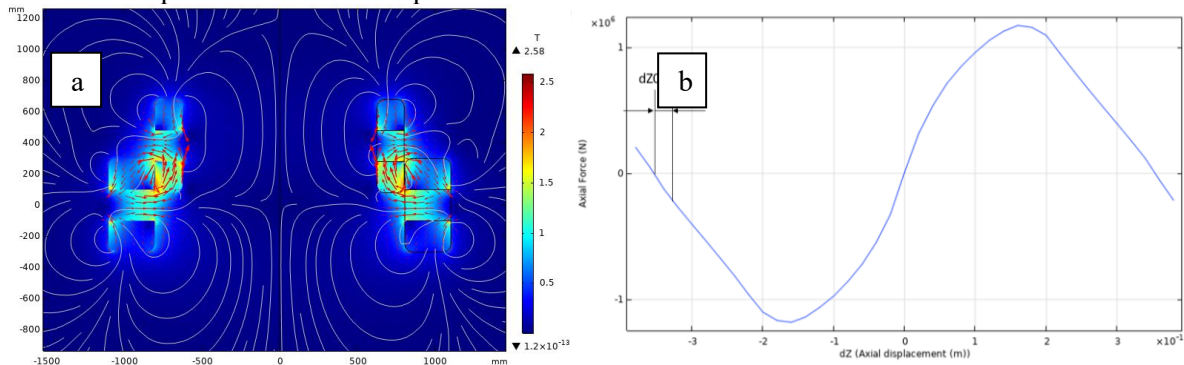

Figure 13. Plot of the axial PMB h_0 h_1 0.2 m, c 4 mm, (a) magnetic flux density (b) axial force-displacement range dZ -0.38 to 0.38 m
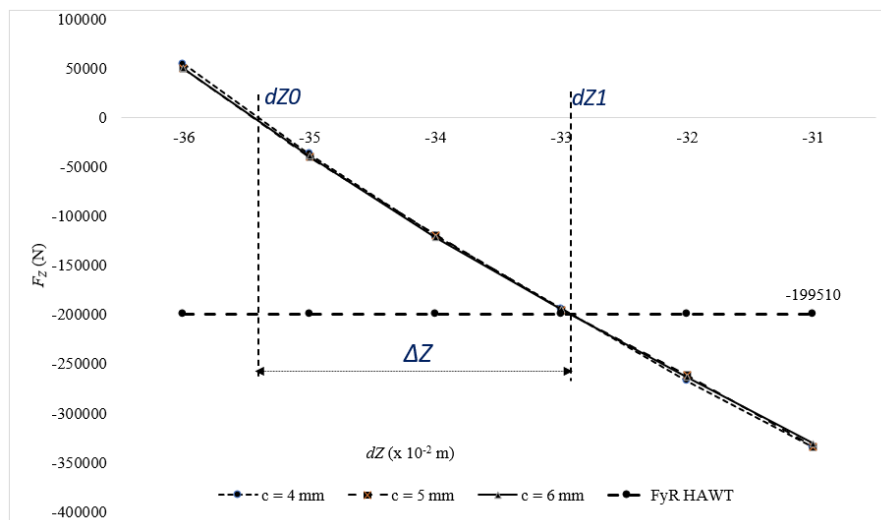

Figure 14. Plot of the axial force -displacement of axial PMB, with h 0.2 m

Figure 14 displays the plot of axial force versus displacement of the axial PMB simulation with a magnetic thickness of 0.2 m, a magnetic gap "c" (4mm; 5mm; 6mm), and a distance set dZ –360mm to -310mm. The distance between the rotor and the stator generates 0N magnetic axial force ($LZ0$) is 354 mm. The HAWT thrust force of 199.5 kN was sustained by axial PMB at c 4mm with displacement ΔZ 25mm, while at c 5 and 6mm, the displacement ΔZ was 26mm. The simulation results show that the thicker the PMB axial magnet, the greater the axial magnetic force.

The Magnetic axial force (F_z) from axial displacement (dZ) in the PMB axial design varied with the magnetic gap and magnetic thickness simulated using the finite element method. The magnetic thrust force must meet 199.5kN and the lowest displacement (ΔZ) in each configuration are limitations into consideration in selecting the PMB axial for the main shaft of the HAWT. Therefore, the axial PMB with magnet thickness, h_0-h_1 of 0.15m, air gap of 4mm produces F_z value 199.5kN, with a minimum ΔZ value 22mm, which is the optimal configuration to obtain the lowest displacement as the HAWT axial bearing. Figure 15 depicts the smallest ΔZ displacement (22mm) in h1.5c4 and h1.5c5 variants, which are PMB axial designs with a thickness of 0.15m and a magnetic gap between the rotor and stator of 4 mm and 5 mm, respectively. Although ΔZ 22mm is the smallest, the flexibility range is still too wide to be utilized as a single substitute for HAWT's mechanical thrust bearing.
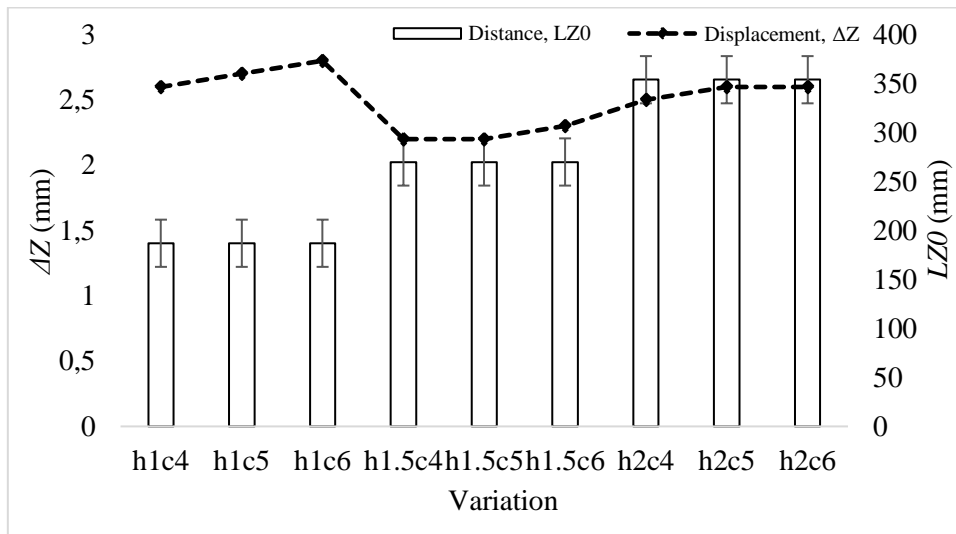
Figure 15. Displacement *ΔZ* and distance *LZ0* of the axial PMB variations
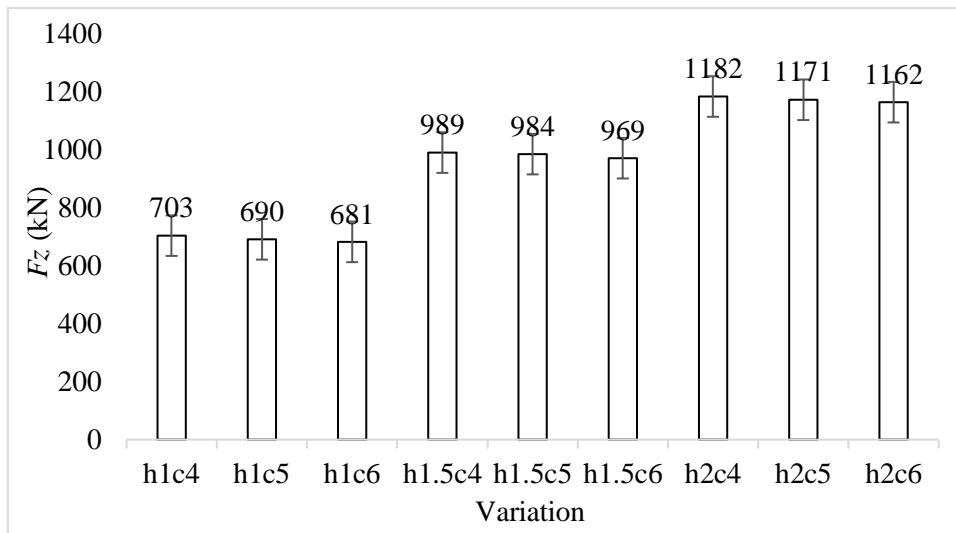

Figure 16. The maximum of magnetic of the axial PMB variations

Figure 15 depicts the *LZ0* distance of 187mm on the Axial PMB 0.1m magnet thickness for the three magnetic gap changes (4,5,6mm), 270mm distance at 0.15m thickness, and 354mm distance at 0.2m thickness. The 0.1m magnet thickness has the lowest *LZ0* value. This demonstrates that the greater the thickness of the PMB axial magnet design, the greater the displacement that provides zero axial magnetic force, but is unaffected by changes in the magnetic gap (c). The rise in displacement value is proportional to the axial magnetic force produced, which increases with the size of the magnet's thickness (see Figure 16). However, there is small decrease produce in the axial magnetic force wherein the size of the magnetic gap (c) gets large. This result is similar to studies in that a smaller magnetic gap width will produce a higher magnetic force [29-30]. The effect of axial magnetic force fluctuation from magnetic gap variation is insignificant, with a difference of 3.16 % for axial PMB with a thickness of 0.1m, a difference of 2 % for a magnet thickness of 0.15m, and a difference of 1.69% for a magnet thickness of 0.2m.

4. Conclusions
The permanent magnetic bearing as an axial bearing of the main shaft HAWT was designed to generate the magnetic force that resists the thrust forces from wind imposed on the rotor blades. The PMB model

consists of rotor and stator magnets arranged in 3 layers that vary in thickness and width of the gap has been simulated base on the displacement of the rotor magnet against the stator. The PMB model with a thickness of 0.15m and a gap of 4mm has the shortest displacement, ΔZ (22mm) that produces a minimum axial magnetic force of 199.5 kN compared to other variations. However, this displacement has a considerable distance, so it is not feasible to use it as a single replacement for HAWT's axial bearing unless combined with the HAWT shaft main bearing close to the rotor. It is also feasible to decrease axial displacement by increasing the number of PMB axial models in one main axis of the HAWT. Analysis shows that the greater the magnet thickness of the PMB, the greater the magnetic axial force and the displacement that provides zero axial magnetic force. Furthermore, increasing the size of the rotor magnet gap towards the stator decreases the magnetic force even though small. The insignificant decrease in the value of the axial force is due to the variation of small gap magnet width in one magnet thickness. The highest decrease was found of the PMB model with a 0.1m thick magnet, where the magnetic force generated at a 4mm magnet gap compared to a 6mm magnetic gap decreased by 3.16%.

References
[1]   Gong, X. dan Q, Wei. 2011. Bearing Fault Detection For Direct-Drive Wind Turbines via Stator Current Spectrum Analysis. IEEE, 11: 313-318.
[2]   Tazi, N., E. Châtelet., dan Y. Bouzidi. 2017. Wear analysis of wind turbine bearings. International Journal of Renewable Energy Research 7(4): 2120.
[3]   Fekry, M., A.M. Mohamed., M. Fanni. dan S. Yoshida. 2019. A Comprehensive performance assessment of the integration of magnetic bearings with horizontal axis wind turbine. Mathematics and Computers in Simulation, 156: 1–39.
[4]   Zhang, W. dan H. Zhu. 2017. Radial magnetic bearings: An overview, Results in Physics, 7: 3756–3766.
[5]   Jin, C., Y. Xu., Z. Jin. dan C. Cheng. 2016. Active Magnetic Bearings Stiffness and Damping Identification from Frequency Characteristics of Control System. Shock and Vibration, 2016: 1-8.
[6]   Yaghoubi, H. 2013. The Most Important Maglev Applications. Journal of Engineering technology 2013:1-19.
[7]   Micha, P. T., T. Mohan. dan S. Sivamani. 2017. Design and Analysis of a Permanent Magnetic Bearing for Vertical Axis Small Wind Turbine. Energy Procedia, 117: 291–298.
[8]   Kriswanto and Jamari, 2016. Radial Forces Analysis and Rotational Speed Test of Radial Permanent Magnetic Bearing For Horizontal Axis Wind Turbine Applications", AIP Conference Proceedings 1725, 020034 1-10
[9]   Daniel DV, Tănase N, Apostol ES, Chiriţă I and Ilie C, "An overview regarding the analytical vs. numerical computation for a PMB used for FESS," 2017 10th International Symposium on Advanced Topics in Electrical Engineering (ATEE), 2017, pp. 458-462
[10]   Teng, W., X, Ding., X. Zhang., L. Y. Liu. Dan Z. Ma. 2016. Multi-fault detection and failure analysis of wind turbine gearbox using complex wavelet transform. Renewable Energy, 93: 591-598.
[11]   Bekinal. S. I. and M. Doddamani. 2020. Friction-Free Permanent Magnet Bearings for Rotating Shafts : A Comprehensive Review. Progress In Electromagnetics Research C. 104: 171–186
[12]   Parambil, L. K. 2019. Design methodology for monolithic layer radial passive magnetic bearing. Journal of Engineering Tribology, 0(0): 1-9.
[13]   Zhang, L., H. Wu., P. Li., Y. Hu. and C. Song. 2019. Design, analysis, and experiment of multiring permanent magnet bearings by means of equally distributed sequences based Monte Carlo method," Mathematical Problems in Engineering, 2019:1-18.
[14]   Wang R, Han T, Wang W, Xue Y, and Fu D. 2018. Fracture analysis and improvement of the main shaft of wind turbine based on finite element method. Advances in Mechanical Engineering. Vol. 10 pp1–9

[15] Anonymous. 2021. Ovako 34CrNiMo6 SB9205 Steel. http://www.matweb.com/search/DataSheet.aspx?MatGUID=e3376bb4f6ab4d9ba23f4b7aa7f1882a&ckck=1

[16] Ni, Q., K. Feng., K. Wang., B. Yang. dan Y. Wang. 2017. A case study of sample entropy analysis to the fault detection of bearing in wind turbine. Case Studies in Engineering Failure Analysis. 9: 99–111.

[17] Ge, Y and Wang. K. (2018). Influence of Microalloying Element on the Microstructure and Mechanical Properties of 34CrNiMo6 Steel for Wind Turbine Main Shaft. Advance in Material Science and Engineering, vol. 2018, 1-6.

[18] Huang CP, Lin X, Liu FC, Cao J, Liu FCG, and Huang WD. 2016. Effects of cooling condition on microstructure and mechanical properties in laser rapid forming of 34CrNiMo6 thin-wall component. Int J Adv Manuf Technol 2016 Vol 82 pp.1269–79,

[19] Branco R, Costa JD, Berto F, Kotousov A, and Antunes FV. 2020. Fatigue crack initiation behaviour of notched 34CrNiMo6 steel bars under proportional bending-torsion loading. Int J Fatigue Vol 130

[20] Veritas DN. 2002. *Design of Wind Turbines*. 2 edition. Norwegia: Det Norske Veritas & Risø National Laboratory.

[21] Ramlan., Muljadi., P. Sardjono., F. Gulo., D. Setiabudidaya. 2016. Crystal Structure and Magnetic Properties of Nd2Fe14B Powder Prepared by Using High Energy Milling from Elements Metal Nd,Fe,B Powders. Journal of Physics, 776:1-6

[22] Suprapedi, Sardjono P, and Muljadi. 2016. Physical and magnetic properties, microstructure of bonded magnet NdFeB prepared by using synthesis rubber. Journal of Physics: Conference Series. 776. 012015

[23] Wang, X., Zhu, K., Li, W., Xu, J., Ali, Z., & Hou, Y. 2020. Nd2Fe14B hard magnetic powders: chemical synthesis and mechanism of coercivity. Journal of Magnetism and Magnetic Materials Vol. 518 pp1-6.

[24] Jeong, J. H., Ma, H. X., Kim, D., Kim, C. W., Kim, I. H., Ahn, J. W., … Kang, Y. S. 2016. Chemical synthesis of Nd2Fe14B hard phase magnetic nanoparticles with an enhanced coercivity value: effect of CaH2 amount on the magnetic properties. New Journal of Chemistry, Vol 40, 10181–10186.

[25] Krugel G, Körner W, Daniel FU, Gutfleisch O and Elsässer C. 2019. High-Throughput Screening of Rare-Earth-Lean Intermetallic 1-13-X Compounds for Good Hard-Magnetic Properties. Metals. Vol 9. pp. 1-13.

[26] Constantinides, S., and J. D. Leon. (2017). Permanent Magnet Materials and Current Challenges Development of Magnet Materials. Arnold Magnetic Technology, Denmark.

[27] Schroeter, H. (2007). Permanent Magnets Materials and Magnet Systems. IBS Magnet, Berlin.

[28] Bekinal, S. I., T. R. Anil. dan S. Jana. 2012. Analysis Of Axially Magnetized Permanent Magnet Bearing Characteristics. Progress In Electromagnetics Research B. 44: 327–343.

[29] Micha PT, Mohan T. and Sivamani S. 2017. Design and Analysis of a Permanent Magnetic Bearing for Vertical Axis Small Wind Turbine. Energy Procedia. Vol 117 pp 291-298.

[30] Zhang L, Wu H, Li P, Hu Y, and Song C.2019. Design, Analysis, and Experiment of Multiring Permanent Magnet Bearings by Means of Equally Distributed Sequences Based Monte Carlo Method, Mathematical Problems in Engineering, Vol. 2019, pp 1-17.

2. Bukti konfirmasi review dan hasil review pertama (28 Oktober 2021)

UNNES
UNIVERSITAS NEGERI SEMARANG

Kriswanto Unnes <kriswanto@mail.unnes.ac.id>

[J. Adv. Res. Fluid Mech. Therm. Sc.] Editor Decision
2 messages

Nor Azwadi <azwadi@semarakilmu.com.my>   Thu, Oct 28, 2021 at 9:09 PM
To: Kriswanto <kriswanto@mail.unnes.ac.id>

Kriswanto:

We have reached a decision regarding your submission to Journal of Advanced Research in Fluid Mechanics and Thermal Sciences, "EIC-Analysis of an Axial Permanent Magnetic Bearing for 1MW Horizontal Axis Wind Turbine ".

Our decision is: Revisions Required

Please submit the revised article by 15 Nov 2021

Editorial Comments:

Please cite few articles from

http://www.akademiabaru.com/submit/index.php/araset

http://www.akademiabaru.com/submit/index.php/cfdl

http://www.akademiabaru.com/submit/index.php/armne

http://www.akademiabaru.com/submit/index.php/arnht

http://www.akademiabaru.com/submit/index.php/arefmht

http://www.akademiabaru.com/submit/index.php/aram

Reviewer A:

Grammar and Spelling:

No language mistakes. Good sentence and paragraph structure and transitions.

Abstract:

Abstract section is excellently written. The abstract has all the required elements (as stated below) that are connected properly.
1. Introduction
2. Aims/objective
3. Methodology
4. Results
5. Discussion

Quality of Tables and Figures:

Tables and figures have excellent clarity and numbered. All tables and figures are mentioned in text and properly discussed.

Conclusion:

Conclusion related to objective. Well written.

References:

As a reminder, please cite related and latest references within 5 years of study since, the year of study is not clarified in the journal.

Recommendation: Revisions Required

_____
Journal of Advanced Research in Fluid Mechanics and Thermal Sciences

---

Kriswanto Unnes <kriswanto@mail.unnes.ac.id>   Sat, Nov 13, 2021 at 8:54 PM
To: Nor Azwadi <azwadi@semarakilmu.com.my>

Ok, I will do it. Thank you for the information on the results of the review and suggestions.
I have cited several articles according to the editor's suggestion, including:
1. https://akademiabaru.com/submit/index.php/araset/article/view/1954/1530
Azizan A, Israr, H A, and Tamin M N. (2020). Effect of Fiber Misalignment on Tensile Response of Unidirectional CFRP Composite Lamina. Journal of Advanced Research in Applied Sciences and Engineering Technology, 11(1), 23–30.
2. https://www.akademiabaru.com/submit/index.php/araset/article/view/1942/1523
J. Ibrahim, M I, and Mohamed Yusoff M Z. (2020). Optimization of Interlocking Structures Made of Flax Fibre Composites to Improve Its Energy Absorption Capability. Journal of Advanced Research in Applied Sciences and Engineering Technology, 10(1), 1–17
3. https://www.akademiabaru.com/submit/index.php/cfdl/article/view/3141/2175
Nasri, W. ., Djebali, . R. ., Goodarzi, M. ., Abbassi, M. A. ., & Abboudi, S. . (2021). Apple Convective Drying - Part I: Finite Elements Parametric Study for Appraising the Operating Conditions Effects. CFD Letters, 11(3), 28–41.
Thanks a lot

Best regards
Kriswanto
[Quoted text hidden]

📄 **SemarakIlmu_PMB Artikel.docx**
1411K

Konfirmasi review di OJS SEMARAK ILMU

Screenshot 1

Notifications ✕

[J. Adv. Res. Fluid Mech. Therm. Sc.] Editor Decision

2021-10-28 02:09 PM

Kriswanto:

We have reached a decision regarding your submission to Journal of Advanced Research in Fluid Mechanics and Thermal Sciences, "EIC-Analysis of an Axial Permanent Magnetic Bearing for 1MW Horizontal Axis Wind Turbine ".

Our decision is: Revisions Required

Please submit the revised article by 15 Nov 2021

Editorial Comments:

Please cite few articles from

http://www.akademiabaru.com/submit/index.php/araset

http://www.akademiabaru.com/submit/index.php/cfdl

http://www.akademiabaru.com/submit/index.php/armne

http://www.akademiabaru.com/submit/index.php/arnht

http://www.akademiabaru.com/submit/index.php/arefmht

Screenshot 2

http://www.akademiabaru.com/submit/index.php/aram

Reviewer A:

Grammar and Spelling:

No language mistakes. Good sentence and paragraph structure and transitions.

Abstract:

Abstract section is excellently written. The abstract has all the required elements (as stated below) that are connected properly.
1. Introduction
2. Aims/objective
3. Methodology
4. Results
5. Discussion

Quality of Tables and Figures:

Tables and figures have excellent clarity and numbered. All tables and figures are mentioned in text and properly discussed.

Conclusion:

Conclusion related to objective. Well written.

References:

As a reminder, please cite related and latest references within 5 years of study since, the year of study is not clarified in the journal.

Recommendation: Revisions Required

3. **Bukti konfirmasi submit revisi, respon kepada reviewer, dan artikel yang diresubmit (13 November 2021)**

Recommendation: Revisions Required

Journal of Advanced Research in Fluid Mechanics and Thermal Sciences

---

Kriswanto Unnes <kriswanto@mail.unnes.ac.id>   Sat, Nov 13, 2021 at 8:54 PM
To: Nor Azwadi <azwadi@semarakilmu.com.my>

Ok, I will do it. Thank you for the information on the results of the review and suggestions.
I have cited several articles according to the editor's suggestion, including:
1. https://akademiabaru.com/submit/index.php/araset/article/view/1954/1530
Azizan A, Israr, H A, and Tamin M N. (2020). Effect of Fiber Misalignment on Tensile Response of Unidirectional CFRP
Composite Lamina. Journal of Advanced Research in Applied Sciences and Engineering Technology, 11(1), 23–30.
2. https://www.akademiabaru.com/submit/index.php/araset/article/view/1942/1523
J. Ibrahim, M I, and Mohamed Yusoff M Z. (2020). Optimization of Interlocking Structures Made of Flax Fibre Composites to
Improve Its Energy Absorption Capability. Journal of Advanced Research in Applied Sciences and Engineering Technology,
10(1), 1–17
3. https://www.akademiabaru.com/submit/index.php/cfdl/article/view/3141/2175
Nasri, W. ., Djebali, . R. ., Goodarzi, M. ., Abbassi, M. A. ., & Abboudi, S. . (2021). Apple Convective Drying - Part I: Finite
Elements Parametric Study for Appraising the Operating Conditions Effects. CFD Letters, 11(3), 28–41.
Thanks a lot

Best regards
Kriswanto
[Quoted text hidden]

📄 **SemarakIlmu_PMB Artikel.docx**
1411K

Konfirmasi submit revisi di OJS SEMARAK ILMU

The article has been revised.

Participants _Edit_

Nor Azwadi (norazwadi)

Kriswanto (kriswanto)

Messages

Note	From
Thank you for the information on the results of the review and suggestions. I have cited several articles according to the editor's suggestion, including: 1. https://akademiabaru.com/submit/index.php/araset/article/view/1954/1530 Azizan A, Israr, H A, and Tamin M N. (2020). Effect of Fiber Misalignment on Tensile Response of Unidirectional CFRP Composite Lamina. Journal of Advanced Research in Applied Sciences and Engineering Technology, 11(1), 23–30. 2. https://www.akademiabaru.com/submit/index.php/araset/article/view/1942/1523 J. Ibrahim, M I, and Mohamed Yusoff M Z. (2020). Optimization of Interlocking Structures Made of Flax Fibre Composites to Improve Its Energy Absorption Capability. Journal of Advanced Research in Applied Sciences and Engineering Technology, 10(1), 1–17 3. https://www.akademiabaru.com/submit/index.php/cfdl/article/view/3141/2175 Nasri, W. ., Djebali, R. ., Goodarzi, M. ., Abbassi, M. A. ., & Abboudi, S. . (2021). Apple Convective Drying - Part I: Finite Elements Parametric Study for Appraising the Operating Conditions Effects. CFD Letters, 11(3), 28–41. Thanks a lot Best regards Kriswanto	kriswanto 2021-11-13 02:03 PM

Add Message

[J. Adv. Res. Fluid Mech. Therm. Sc.] Editor Decision	2021-10-28 02:09 PM
[J. Adv. Res. Fluid Mech. Therm. Sc.] Editor Decision	2021-11-14 05:02 AM
[J. Adv. Res. Fluid Mech. Therm. Sc.] Editor Decision	2022-04-22 06:30 AM

Reviewer's Attachments   Q Search

No Files

Revisions   Q Search   Upload File

▸ 242 SemarakIlmu_PMB Artikel.docx   November 13, 2021   Article Text

Review Discussions   Add discussion

Name	From	Last Reply	Replies	Closed
▸ The article has been revised.	kriswanto 2021-11-13 02:03 PM	-	0	☐

Analysis of an Axial Permanent Magnetic Bearing for 1MW Horizontal Axis Wind

Kriswanto[1,*], Rizqi Fitri Nuryanto[1], Renaldy Prasdiansyah[1], Dony Hidayat Al-Janan[1], Widya Aryadi[1], Ahmad Roziqin[1], Samsudin Anis[1], Wirawan Sumbodo[1], and Jamari[2]

*kriswanto@mail.unnes.ac.id

[1] Department of Mechanical Engineering, Universitas Negeri Semarang, Gd E9 Kampus Sekaran Gunungpati, Semarang, Indonesia

[2] Department of Mechanical Engineering, University of Diponegoro, Jl. Prof. Sudharto Kampus UNDIP Tembalang, Semarang 50275, Indonesia

ARTICLE INFO	ABSTRACT
	One way to reduce maintenance costs while improving wind turbine efficiency is to replace mechanical bearings with permanent magnetic bearings. The permanent magnetic bearing is a free contact bearing in which the rotor is elevated from the stator by the magnet's repelling force. The purpose of this study is to analyze the variation of permanent magnet width and the gap distance between the rotor-stator magnets that can produce the magnetic axial force opposing the thrust force of 1MW horizontal axis wind turbines (HAWT). The method used in this study is a magnetic force simulation using finite element method by varying the magnet thickness, width of the gap, and displacement between the rotor-stator of the PMB model. The PMB model consists of rotor and stator magnets arranged in 3 layers with Nd2Fe14B type material with a magnetic flux density of 1.45 T. Variations in thickness of the rotor and stator magnets are 0.1; 0.15, respectively; 0.2 (m), while variations in the width of the magnetic gap are 4, 5, 6 (mm). The results of the study found that the displacement that produces an axial magnetic force that can support a thrust force of 199.5kN is the lowest in the PMB model with a magnetic thickness of 0.15m with a magnetic gap of 4mm, while the highest is at a magnetic thickness of 0.1m with a magnet gap of 6mm. The greater the thickness of the PMB axial magnet design, the greater the displacement that provides zero axial magnetic forces. Further, the maximum of the magnetic axial force is rise on with increasing magnet thickness.

1. Introduction

One of the most critical components of wind turbines is the bearing. Furthermore, the wind industry has recognized main bearing failures as a major concern in terms of raising wind turbine reliability and availability, according to the European Academy of Wind Energy (EAWE) [1]. It is due to the high maintenance costs and long periods of downtime related to main bearing failures. Large-scale power plants currently apply mechanical bearings for onshore and offshore wind turbines. Nevertheless, the use of it has a limited-service life as well as capability [2]. So the effort to improve the efficiency and reliability of wind turbines is to minimize friction using magnetic bearings [3]. The

magnetic bearing is a bearing that utilizes refuse forces to support a rotor without physical contact [4].

Magnetic bearings have the benefit of being able to adapt to changing operating conditions and the environment. Within certain limits, the adjustment of magnetic bearing caused vibration was independent of the rotor position. Moreover, magnetic bearings can maintain rotor equilibrium positions at various loads. The rotor can rotate on its main axis and does not cause vibration on the foundation. Due to the levitation force of magnets, the vibration was significantly reduced [5]. The study of the magnetic bearing on the flywheel has the same polarity as the rotor, generating repulsive forces that keep the flywheel magnetically levitating and thereby reducing friction losses inside [6]. Nevertheless, permanent magnetic bearings (PMB) have several problems, including stability problems. Otherwise, given the long lifetime of its use then PMB is an effective solution to overcome the bearing problems [7]. The study of PMB in wind turbine prototypes to substitute mechanical bearings can enhance rotational speed and torque, therefore enhancing Horizontal Axis Wind Turbine (HAWT) performance [8]. Comparative study of axial force results of PMB between analytical approach and finite element method shows good agreement between the two [9]

The permanent magnetic bearing has been applied for rotating shafts that are used to replace conventional bearings which have high maintenance costs and friction [11]. Therefore, maintenance costs of wind turbines can be minimized by the use of permanent magnetic bearings. It is aligned with the statement that passive magnetic bearing is one of the most economical and effective methods to lift the two surfaces in relative motion that do not require active control and additional energy [12].

The study of modeling of the axial permanent magnetic bearing that comparing the theoretical simulation of the Monte Carlo method and the finite element method found that errors approximate zero and are consistent. Moreover, the experimental results are consistent with the simulation analysis [13]. The previous study [3-8][10-12] shows the permanent magnetic bearings reduce friction, minimizes maintenance costs, can replace mechanical bearings. While none of the above literature has developed or studied the axial force of a PMB for a 1MW HAWT. The main shaft bearing of the HAWT must support both radial and axial loads (thrust forces). Furthermore, the HAWT thrust force is affected by the cut in and cut out of wind speed. The higher the wind speed, the higher the axial load on the main shaft bearing HAWT. Therefore, this paper presents to analyzes the axial magnetic force of the several thicknesses and air gaps of the permanent magnetic bearing models as the main bearing of the 1MW HAWT. Magnetic force and displacement are analyzed to find the shortest gap that can sustain the highest thrust force (at the cut out of wind speed). The main bearing locates near the gearbox, as shown in Figure 1 and indicated by number 2.
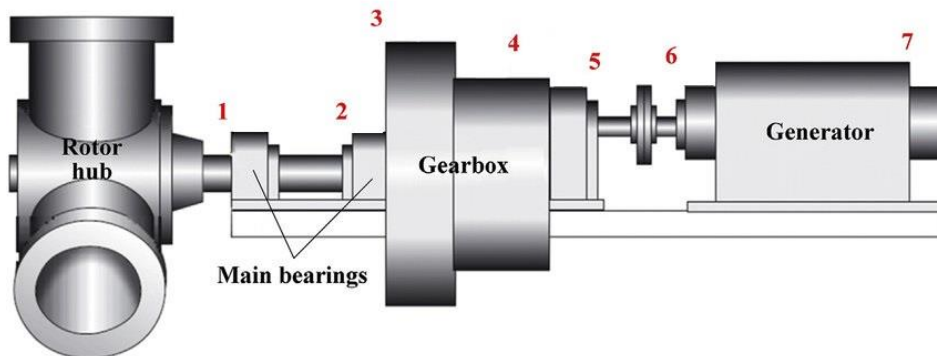

Fig. 1. Main shaft bearings [10]

2. Methodology

The main shaft of the HAWT model, made of 34CrNiMo6 steel, complies with wind turbine certification standards [14]. Furthermore, it was analyzed by finite element method and confirmed by Mohr II theory calculations to get the deflection value due to radial load. The defection will be used as the minimum air gap to prevent collisions between the rotor magnets and the stator magnets. The material properties of 34CrNiMo6 steel used in the finite element method are the density of 7800 (kg/m^3), elasticity modulus by 210 GPa, and Poisson's ratio of 0.3 [15]. The main shaft must be safe during operation to prevent damage that causes unexpected economic losses [16]. Furthermore, the 34CrNiMo6 steel has good toughness properties also the shock resistance of the material is good enough in the operating environment temperature [17]. In addition to being applied to wind turbine shafts, 34CrNiMo6 is high-strength structural steel frequently used in large-sized shaft components with complex geometry, such as aircraft propeller shafts and automobile connecting rods [18-19]. The specifications for the horizontal axis wind turbine show in Table 1.

Table 1
HAWT model specifications

Part name	Specification	Value
Rotor Blade	Number of blades	3
	Diameter (m)	54.4
	power coefficient, C_P	0.4877
	Tip Speed Ratio, TSR	2.82
	Rotor Load (N)	164150
Main shaft	Density, ρ (kg/m^3)	7800
	Diameter (m)	1.25
	Massa, m (Kg)	404.3
	Length, l (m)	4.5
	Material	34CrNiMo6
Bearing	Diameter Bore (m)	1.25
	Outer diameter (m)	2.2
	Material	$Nd_2Fe_{14}B$
	Remanent flux density, B_r (T)	1.45
Control	Cut in speed (m/s)	3.5
	Cut out speed (m/s)	15

The maximum deflection is the distance of the shaft to prevent the possibility of friction between the stator magnet and the rotor magnet. This calculation uses two methods, namely the finite element analysis method and Mohr's Theory calculation. Many uses of FEM in the structural field are to analyze stresses and displacements [20-24]. The bending moment diagram on the HAWT main shaft shows in Figure 2.
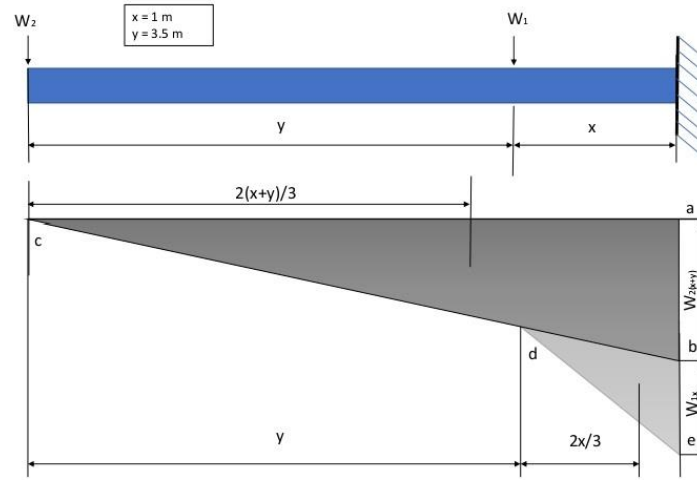
Fig. 2. Bending moment diagram of HAWT main shaft

Which *x* (m) is the distance from the base of the shaft to the center of the magnetic load, y is the distance from the center of gravity to the end shaft (m), W_1 is the rotor magnet load (N), and W_2 is the total load from the connector hub load and the rotor load (N). Hereafter, the equations (1-2) for the deflection calculations.

$$I_P = \pi 4 (r_{c2}{}^4 - r_{c1}{}^4) \tag{1}$$

$$\delta = \frac{1}{EI} \int_X^Y M\, x\, \mathrm{d}x \tag{2}$$

Where I_P is the polar inertia of the shaft, r_{c1} is the inner radius of the shaft cylinder, r_{c2} is the outer radius of the shaft cylinder, *E* modulus of elasticity of 34CrNiMo6, *M* is an area of the bending moment diagram, *x* is the distance of the load to the base of the shaft, and δ is the maximum deflection of the shaft. The data for each variable is present in Table 2.

Table 2
Properties on HAWT main shaft

x [m]	y[m]	W_1 [N]	W_2 [N]	r_{c1} [m]	r_{c2} [m]	E [GPa]
1	3.5	17,283	164,150	0.225	0.625	210

The location of the axial PMB on the HAWT main shaft is shown in Figure 3, wherein the position is closer to the gearbox. The free-body diagram of the force and moment on the main shaft see in Figure 4. The thrust force received by the rotor from the wind calculate using Equation 4.
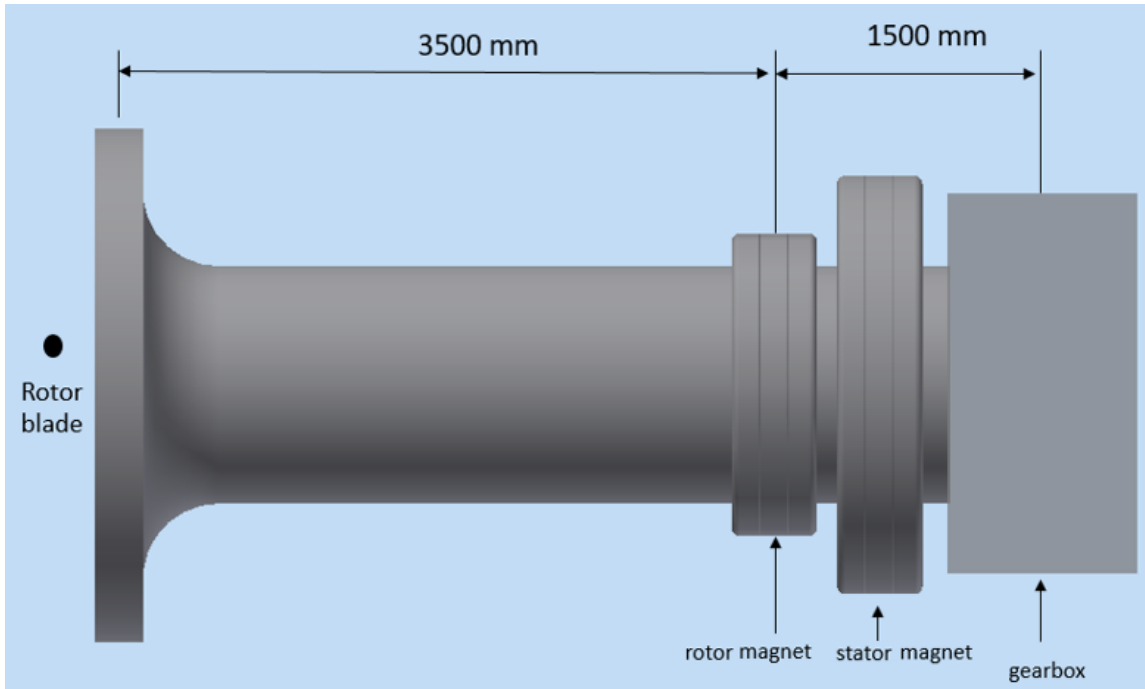
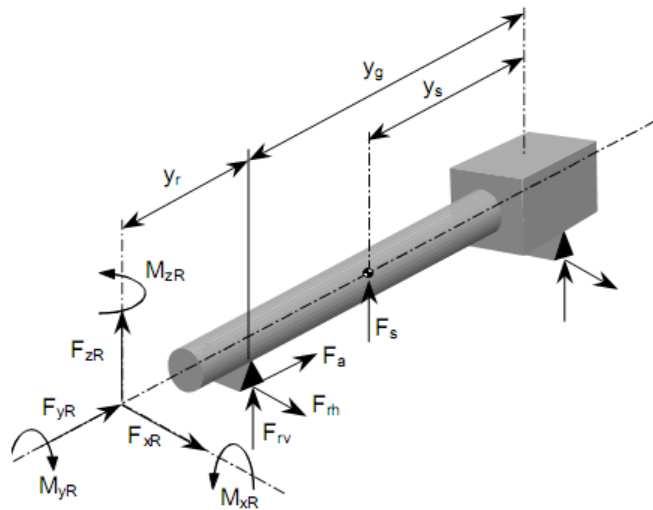**Fig. 3.** Location of axial PMB on the HAWT main shaft

Fig. 4. Forces and moments on the HAWT main shaft [25]

$$A = \pi\, r2 \tag{3}$$

$$F_{yR} = \frac{1}{2}\, \rho\, A\, (v_1^2 - v_2^2) \tag{4}$$

The magnetic force simulation in this study uses the finite element method assisted of COMSOL by integrating vector Equations (5). COMSOL software is a powerful modeling and simulation tool for engineering and industrial applications combining several physics connections [26]. The axial force of the PMB model was simulation by displacement distance between the rotor magnet against the stator.

$$f = n.T = -\frac{1}{2}n(H.B) + (n.H)B^T \tag{5}$$

Where *f* is the magnetic force (n), *n* is the external normal vector, *T* is the tensor stress Maxwell, *H* is the magnetic field/ coercivity, *B* is the magnetic flux density (T).

The magnetic model uses the relationship between the density of the magnetic lines force and the magnetic field, which is expressed by Equation 6.

$$B = \mu_r \mu_0 H \tag{6}$$

Where μ_r is the relative permeability and μ_0 is the absolute magnetic permeability.

Magnetic field using Ampere's law model, with the stationary magnetic field Equation 7.

$$B = \bar{V} A' \tag{7}$$

$$\mu_0^{-1} \mu_r^{-1} \overline{V} A' = J \tag{8}$$

Where $\bar{V}$ is the vector operators, *A'* is the Magnetic potential vector, and J is the magnetization residual or magnetism induction density.

Boundary conditions using the Equation 9.

$$n_1 A' = 0 \tag{9}$$

The magnetic field was the model using a magnetic field interface model. Ampere's law used to include magnetic field physics into all free air domains. The infinite element domain uses to simulate the large region of free space surrounding the magnets. The material for all free domains is air. The free triangular mesh generated in the simulation is both the computational domain and the magnets. In this study, the magnet material made from $Nd_2Fe_{14}B$, which the magnet is composed of a mixture of neodymium (Nd), iron powder (Fe), and boron powders (B) using the high compression molding method [27]. The $Nd_2Fe_{14}B$ is a kind of hard magnet with excellent magnetic characteristics, possesses the highest values of maximum energy product (BH) max and coercivity [28-30]. In addition, $Nd_2Fe_{14}B$ is the strongest permanent magnet because maximum energy reaches more than $400kJ/m^3$ [31-33]. Figure 5 show the HAWT main shaft design, all dimensional units of mm. The diameter of the HAWT main shaft is a limitation in determining the inner diameter of the PMB rotor magnet.
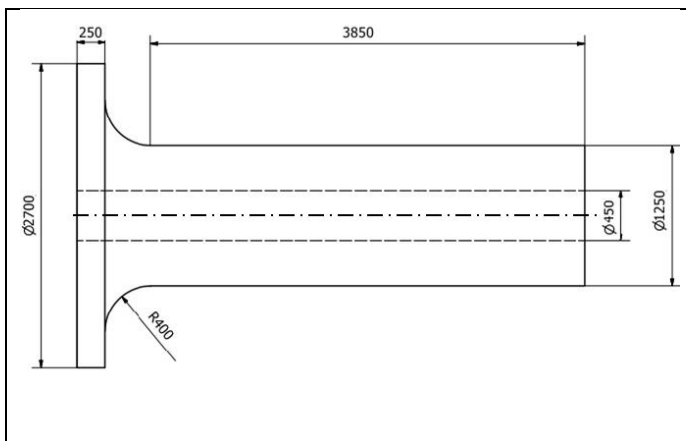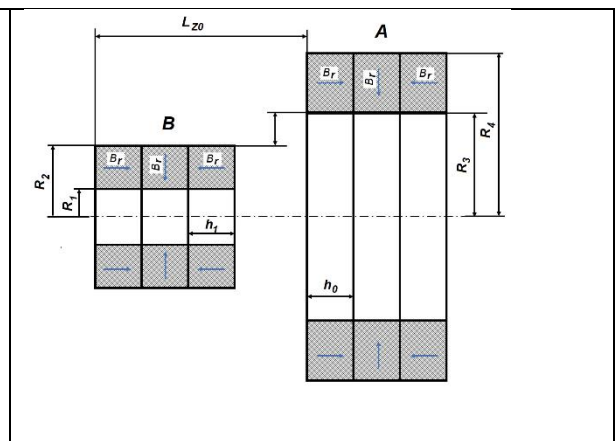
Figure 5. HAWT main shaft design	Figure 6. Design of axial PMB configuration

As illustrated in Figure 6, the PMB axial configuration design includes three magnets on the rotor magnet *B* and the stator magnet *A*, which has a magnetic force density direction like in Figure. The rotor magnet is an inner magnet with an outer diameter smaller than the stator magnet's inner diameter, resulting in a gap. Placement of the rotor magnet against the stator, *LZ0* must be in a condition where there is no axial magnetic force interaction between the two (F_z=0N). This setting is a condition when the wind turbine rotor does not receive thrust force from the wind. Meanwhile, the maximum thrust force or at the cut-out wind speed must restrain by the PMB thrust force with the smallest possible displacement distance (ΔZ).

The design specifications of the axial PMB model are presented in Table 3, wherein the model uses a configuration of concentric ring permanent magnets which have different dimensions and have opposite directions of magnetic force density (*Br*). Furthermore, the axial PMB in the present study functions as the axial main shaft bearing of HAWT.

Table 3
PMB model specifications

	Outer magnet, A	Inner magnet, B
Inner Radius (m)	R_3 = 0.805; 0.806; 0.8067	R_1 = 0.625
Outer Radius (m)	R_4 = 1.1	R_2 = 0.8
Thickness (m)	h_0 = 0.1; 0.15; 0.2	h_1 = 0.1; 0.15; 0.2
Magnetic Flux Density, *Br* (T)	1.45	1.45

3. Results

3.1 Thrust force on the HAWT main shaft

The Thrust force (F_{yR}) of the HAWT main shaft is calculated by equation (3), which A of 2323.098 m^2 and ρ is the air density assumed is 1.293 kg/m^3. The thrust force results on the HAWT main shaft are shown in Figure 7.

The minimum thrust force is 10862.22 N generated at a wind speed of 3.5 m/s at the cut-in of HAWT, while the maximum is 199.5kN generated at a wind speed of 15 m/s, namely at a HAWT cut-out. The higher the wind speed, the higher the thrust force. According to Figure 7, the HAWT main shaft bearing must sustain an thrust force of 199.5 kN .
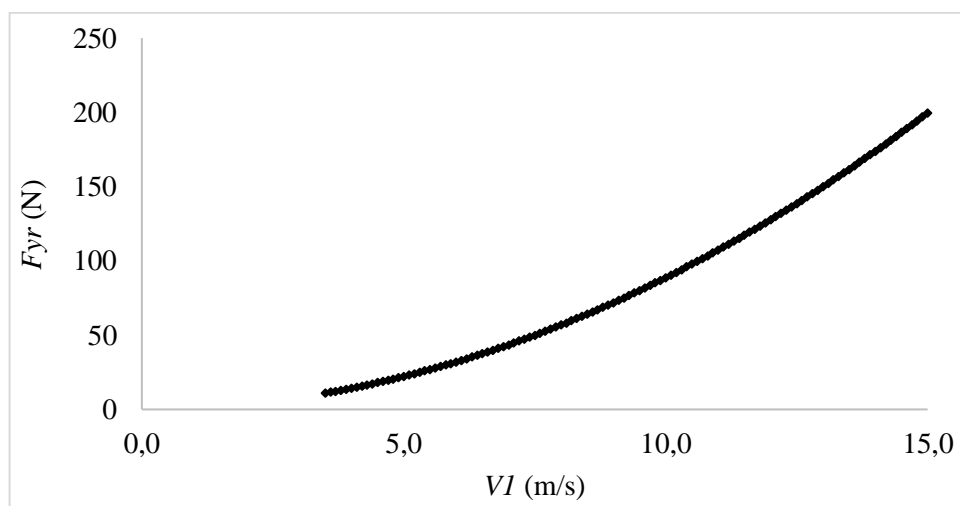

Fig. 7. Graph of the thrust force on the HAWT main shaft vs windspeed

3.2 Maximum deflection on the main shaft of HAWT

The maximum deflection is analyzed to determine the minimum gap between the rotor magnets and the stator not to touch later. The results obtained from the finite element method (FEM) use COMSOL will then compare with mathematical of the Mohr II theoretical equation. The results of the maximum deflection analysis show in Figure 8.
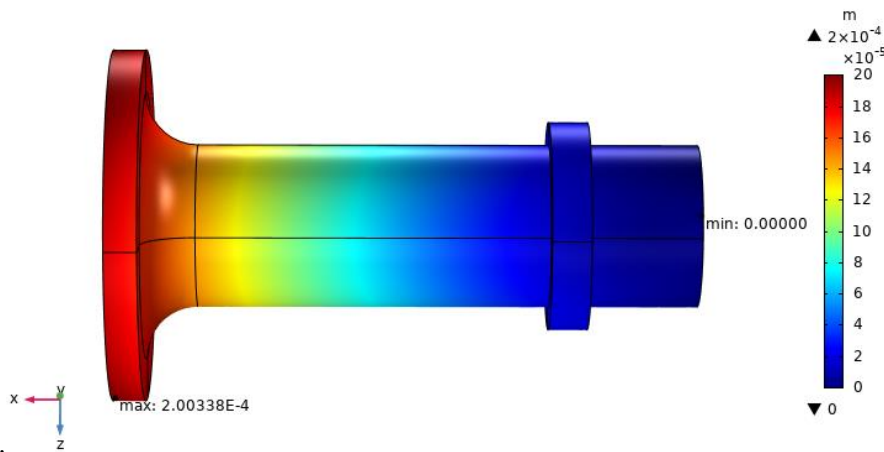

Figure 8. Maximum deflection of HAWT main shaft use FEM

Table 4
Model Validation with Mohr II theory

	FEM	Analytic	Variation (%)
Maximum Deflection (mm)	0.20033	0.20036	0,015

The maximum deflection of the modeling approximates analytic calculations using Mohr II theory (see Table 4). Moreover, the discrepancy between the two methods above has 0.015 %, which indicates that the FEM agrees with the analytic.

3.3 PMB model validation

Figure 8 is a plot of axial force versus displacement generated from the modeling, where the axial force Fz is 126.12 N, is the rotor magnet experiences an of the stator as far as 6mm towards the positive axial direction dZ. This also applies to the displacement that leads to negative axial where at dZ at a distance of -6mm an axial force Fz equal to -126.12 N is produced.
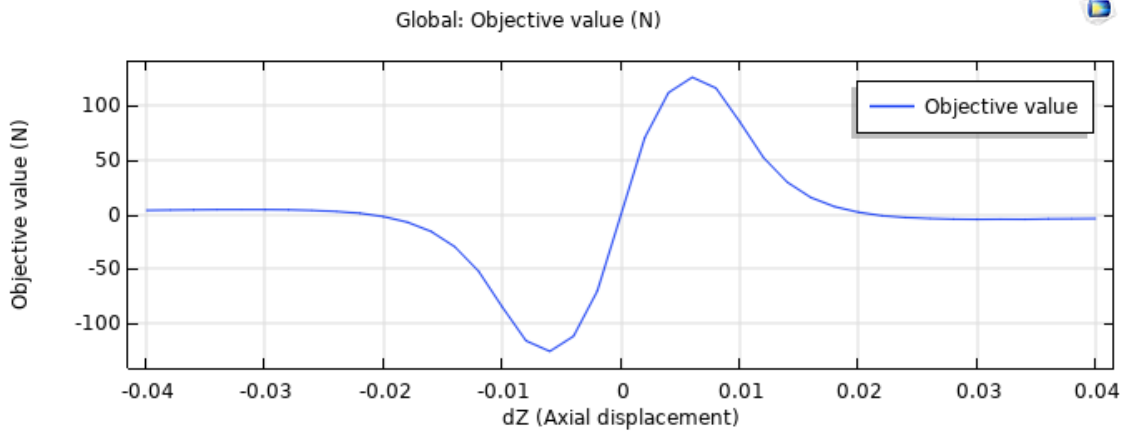
Fig. 9. Plot of the magnetic axial force of the modelling

Table 5
Validation of the axial force with Bekinal model

	Modeling	Bekinal model [34]	Variation (%)
Axial Force (N)	126.12	126.59	0.37

The maximal axial force obtained through modeling is 126.12N, whereas the Bekinal mathematical model yields 126.59N (see Table 5). The discrepancy between the results of the two methods is 0.37%, which indicates that the modeling method is declared valid.

3.4 Axial force modeling of 0.1 m magnet thickness of the PMB

The axial PMB design is depicted in Figure 6, then the parameters provided in Table 1 have values of h_0-h_1 indicate a magnet thickness of 0.1 m. The variation in this configuration lies in the width of the magnetic gap with R_3 values are 0.805, 0.806, 0.807 (m), so that the magnetic gap c becomes 4 mm, 5 mm, and 6 mm. The maximum magnetic flux density of 1.45T (see Figure 10-a) at 0.1 m thickness variation and 4mm gap as shown in the red area concentrated in the center of the magnet both on the rotor and stator. Figure 10-b depicts the axial force towards displacement with dZ – 0.38 m to 0.38 m.
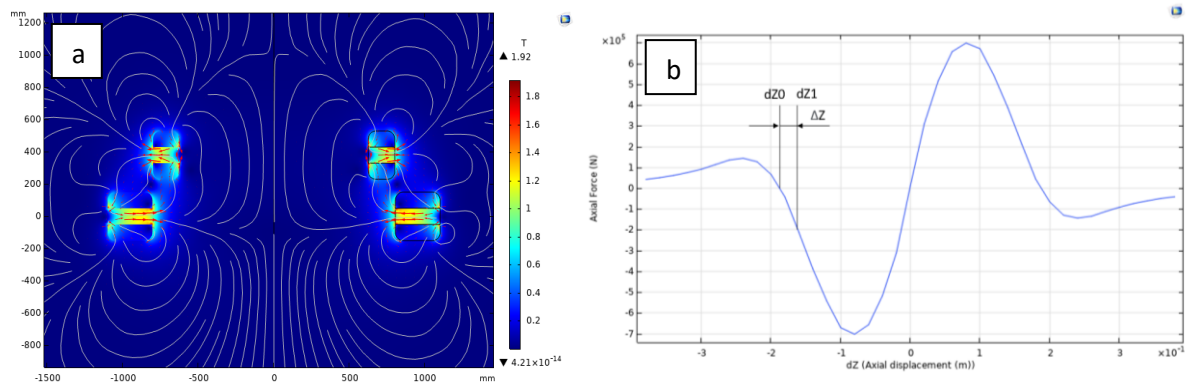

Fig. 10. Plot of the axial PMB h_0 h_1 0.1 m, c 4mm, (a) magnetic flux density (b) axial force-displacement range dZ -0.38 to 0.38 m
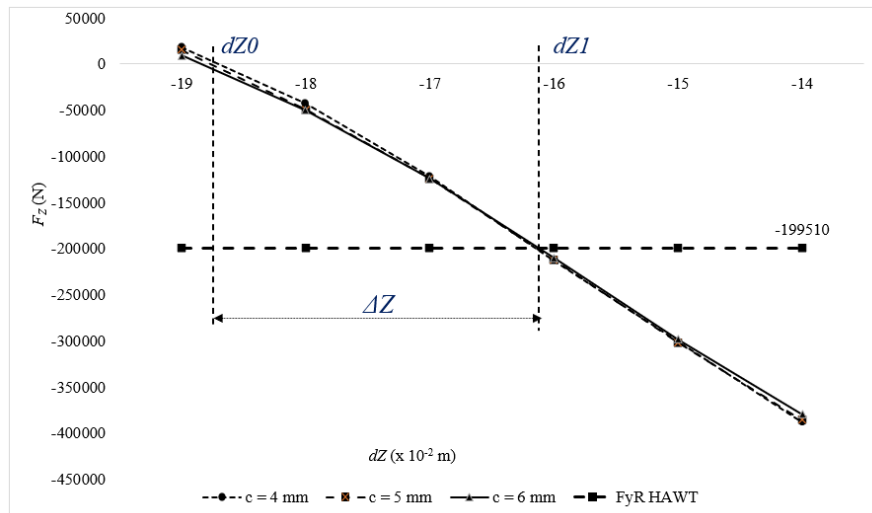
Fig. 11. The plot of the axial force-displacement of axial PMB, with h 0.1 m

Figure 11 is a plot of the axial force versus displacement generated in the axial PMB simulation with a magnetic thickness of 0.1 m which the width is varied for the magnetic gap "c" (4mm; 5mm; and 6mm) and for the distance set at dZ −190mm to -140mm. The rotor-stator distance that produces 0N (*LZ0*) magnetic axial force is 187mm. The measurement of ΔZ starts from the displacement point of the rotor-stator at an axial force of 0N (*dZ0*) to the location (*dZ1*) wherein F_Z 199.5 kN is produced. The thrust force on the HAWT main shaft, which is 199.5 kN, can be supported by axial PMB at *c* 4mm with displacement ΔZ 26mm, *c* 5mm with ΔZ 27mm, and *c* 6mm, the distance ΔZ is 28mm. Based on the simulation results, the minimum displacement against the thrust force is found at c 4mm. Furthermore, this configuration can support the axial load on the HAWT main shaft with a ΔZ value of 2.6mm.

3.5 Axial force modeling of 0.15 m magnet thickness of the PMB

The axial PMB design uses the parameters provided in Table 1 have values of h0-h1 indicate a magnet thickness of 0.15 m. The difference in this configuration magnetic gap *c* values of 4mm, 5mm, and 6mm. Figure 12-a shows the maximum magnetic flux density of 1.45T at 0.15 m thickness variation and 4mm gap, which is centered in the magnet's center on both the rotor and stator. Figure 12-b shows the axial force-displacement which dZ − 0.38 m to 0.38 m.
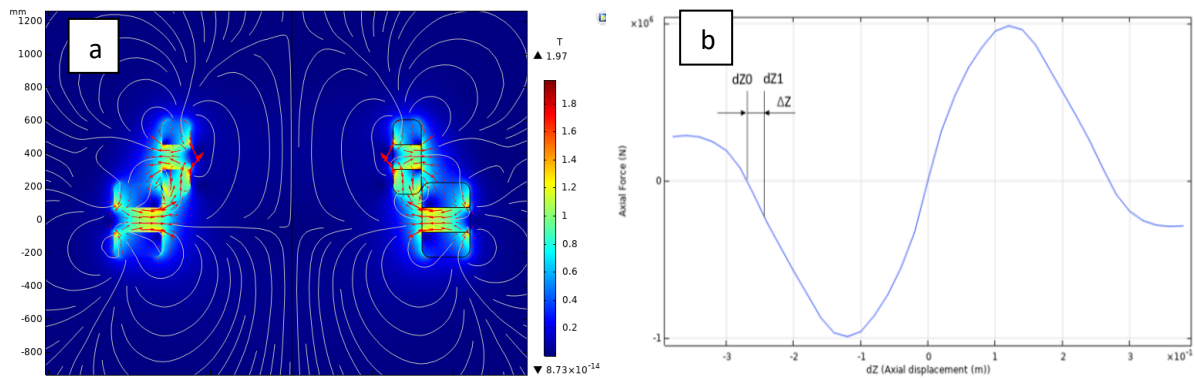

Fig. 12. Plot of the axial PMB h_0 h_1 0.15 m, c 4mm, (a) magnetic flux density (b) axial force-displacement range dZ -0.38 to 0.38 m
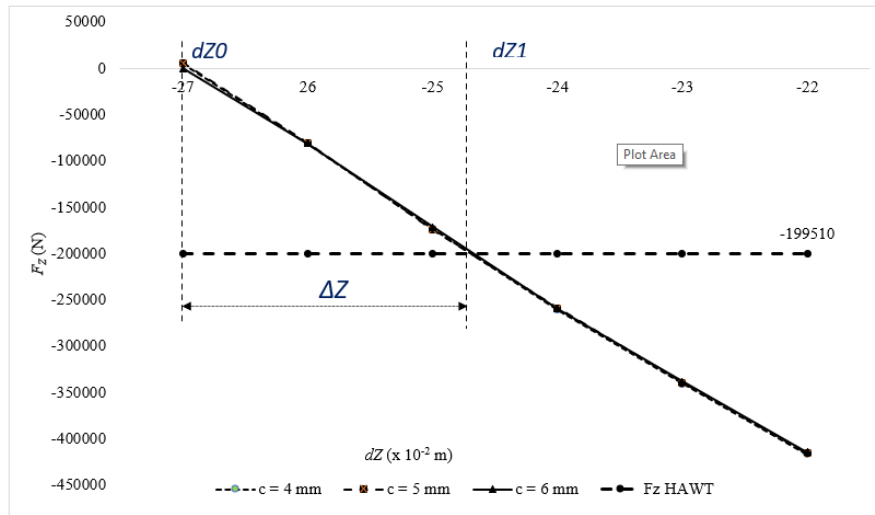
Fig. 13. Plot of the axial force -displacement of axial PMB, with h 0.15 m

Figure 13 shows a plot of the axial force against displacement created in the axial PMB simulation with a magnetic thickness of 0.15 m and a magnetic gap "c" (4mm; 5mm; 6mm) and a distance set at dZ – 270mm to -220mm. The rotor-stator distance required to generate ($LZ0$) 0 N magnetic axial force is 270mm.The thrust force of 199.5 kN on the HAWT main shaft may be sustained by axial PMB at c 4mm with displacement ΔZ 22mm, c 5mm with displacement ΔZ 22mm, and c 6mm with distance ΔZ 23mm. According to the results, the minimum displacement sustain the thrust force is discovered at c 4mm. Furthermore, with a ΔZ value of 22mm, this arrangement can sustain the axial load on the HAWT main shaft. The simulation results of the axial magnetic force at 0.15m thickness of the magnet is similar to 0.1m thickness configuration, wherein the air gap (c) the smaller the displacement smaller too.

3.6 Axial force modeling of 0.2 m magnet thickness of the PMB

The axial PMB design proposes the specifications shown in Table 1, with h_0-h_1 indicating a magnet thickness of 0.2m. The magnetic gap c values of 4mm, 5mm, and 6mm differ in this arrangement. Figure 14-a depicts the maximum magnetic flux density of 1.45T in the central magnetic region of the rotor and stator, for 0.2 m thickness variation and 4mm gap of the axial PMB Design. Figure 14-b depicts the axial force-displacement relationship with dZ – 0.38 m to 0.38 m.
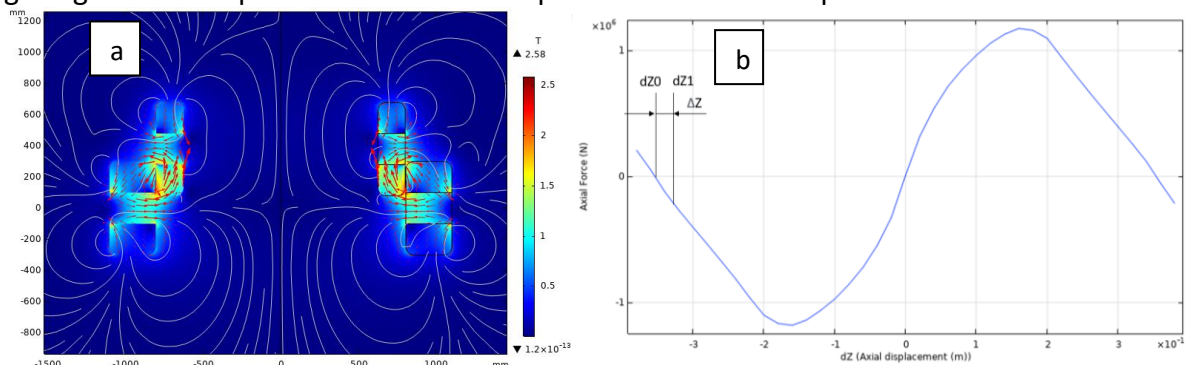

Figure 14. Plot of the axial PMB h_0 h_1 0.2 m, c 4 mm, (a) magnetic flux density (b) axial force-displacement range dZ -0.38 to 0.38 m
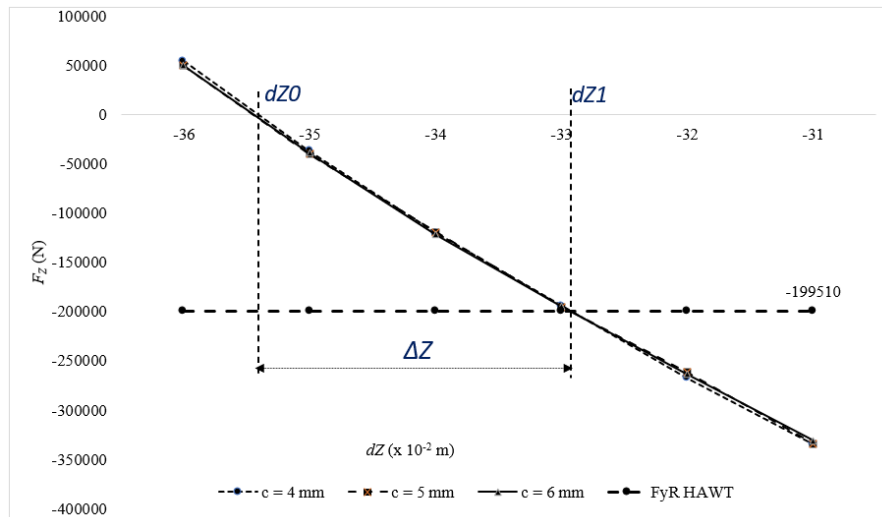
Fig. 15. Plot of the axial force -displacement of axial PMB, with h 0.2 m

Figure 15 displays the plot of axial force versus displacement of the axial PMB simulation with a magnetic thickness of 0.2 m, a magnetic gap "*c*" (4mm; 5mm; 6mm), and a distance set *dZ* –360mm to -310mm. The distance between the rotor and the stator generates 0N magnetic axial force (*LZ0*) is 354 mm. The HAWT thrust force of 199.5 kN was sustained by axial PMB at c 4mm with displacement *ΔZ* 25mm, while at *c* 5 and 6mm, the displacement *ΔZ* was 26mm. The simulation results show that the thicker the PMB axial magnet, the greater the axial magnetic force.

The Magnetic axial force (F_z) from axial displacement (*dZ*) in the PMB axial design varied with the magnetic gap and magnetic thickness simulated using the finite element method. The magnetic thrust force must meet 199.5kN and the lowest displacement (*ΔZ*) in each configuration are limitations into consideration in selecting the PMB axial for the main shaft of the HAWT. Therefore, the axial PMB with magnet thickness, h_0-h_1 of 0.15m, air gap of 4mm produces F_z value 199.5kN, with a minimum *ΔZ* value 22mm, which is the optimal configuration to obtain the lowest displacement as the HAWT axial bearing. Figure 15 depicts the smallest *ΔZ* displacement (22mm) in h1.5c4 and h1.5c5 variants, which are PMB axial designs with a thickness of 0.15m and a magnetic gap between the rotor and stator of 4 mm and 5 mm, respectively. Although *ΔZ* 22mm is the smallest, the flexibility range is still too wide to be utilized as a single substitute for HAWT's mechanical thrust bearing.
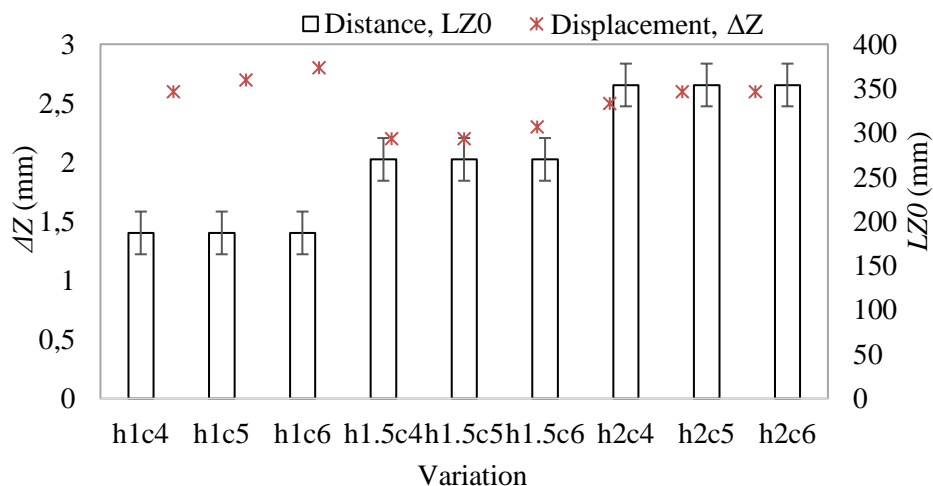

Fig. 16. Displacement *ΔZ* and distance *LZ0* of the axial PMB variations
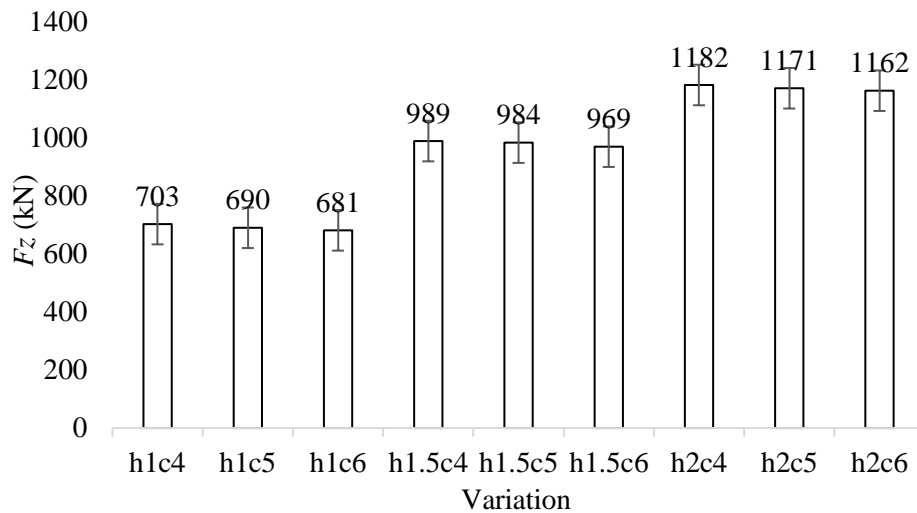
Fig. 17. The maximum of magnetic of the axial PMB variations

Figure 16 depicts the *LZ0* distance of 187mm on the Axial PMB 0.1m magnet thickness for the three magnetic gap changes (4,5,6mm), 270mm distance at 0.15m thickness, and 354mm distance at 0.2m thickness. The 0.1m magnet thickness has the lowest *LZ0* value. This demonstrates that the greater the thickness of the PMB axial magnet design, the greater the displacement that provides zero axial magnetic force, but is unaffected by changes in the magnetic gap (c). The rise in displacement value is proportional to the axial magnetic force produced, which increases with the size of the magnet's thickness (see Figure 17). However, there is small decrease produce in the axial magnetic force wherein the size of the magnetic gap (c) gets large. This result is similar to studies in that a smaller magnetic gap width will produce a higher magnetic force [7,35]. The effect of axial magnetic force fluctuation from magnetic gap variation is insignificant, with a difference of 3.16 % for axial PMB with a thickness of 0.1m, a difference of 2 % for a magnet thickness of 0.15m, and a difference of 1.69% for a magnet thickness of 0.2m.

4. Conclusions

The permanent magnetic bearing as an axial bearing of the main shaft HAWT was designed to generate the magnetic force that resists the thrust forces from wind imposed on the rotor blades. The PMB model consists of rotor and stator magnets arranged in 3 layers that vary in thickness and width of the gap has been simulated base on the displacement of the rotor magnet against the stator. The PMB model with a thickness of 0.15m and a gap of 4mm has the shortest displacement, *ΔZ* (22mm) that produces a minimum axial magnetic force of 199.5 kN compared to other variations. However, this displacement has a considerable distance, so it is not feasible to use it as a single replacement for HAWT's axial bearing unless combined with the HAWT shaft main bearing close to the rotor. It is also feasible to decrease axial displacement by increasing the number of PMB axial models in one main axis of the HAWT. Analysis shows that the greater the magnet thickness of the PMB, the greater the magnetic axial force and the displacement that provides zero axial magnetic force. Furthermore, increasing the size of the rotor magnet gap towards the stator decreases the magnetic force even though small. The insignificant decrease in the value of the axial force is due to the variation of small gap magnet width. The highest decrease was found of the PMB model with a

0.1m thick magnet, where the magnetic force generated at a 4mm magnet gap compared to a 6mm magnetic gap decreased by 3.16%.

References

[1]   Encalada-Davila A, Puruncajas B, Tutiven C, and Vidal Y. 2021. Wind Turbine Main Bearing Fault Prognosis Based Solely on SCADA Data. Sensors 21, no. 6: 2228. https://doi.org/10.3390/s21062228

[2]   Tazi, N., E. Châtelet., and Y. Bouzidi. Wear analysis of wind turbine bearings. International Journal of Renewable Energy Research 7 No 4 (2017): 2120-2129.

[3]   Fekry, M., A.M. Mohamed., M. Fanni. dan S. Yoshida. A Comprehensive performance assessment of the integration of magnetic bearings with horizontal axis wind turbine. Mathematics and Computers in Simulation, 156 (2019): 1–39. https://doi.org/10.1016/j.matcom.2018.06.011

[4]   Zhang, W. and H. Zhu. Radial magnetic bearings: An overview, Results in Physics 7 (2017): 3756–3766. https://doi.org/10.1016/j.rinp.2017.08.043

[5]   Jin, C., Y. Xu., Z. Jin. dan C. Cheng. Active Magnetic Bearings Stiffness and Damping Identification from Frequency Characteristics of Control System. Shock and Vibration, 2016 (2016): 1-8. https://doi.org/10.1155/2016/1067506

[6]   Alami AH. 2021. Introduction to Mechanical Energy Storage, Reference Module in Earth Systems and Environmental Sciences, Elsevier https://doi.org/10.1016/B978-0-12-819723-3.00080-9

[7]   Micha, P. T., T. Mohan. dan S. Sivamani. Design and Analysis of a Permanent Magnetic Bearing for Vertical Axis Small Wind Turbine. Energy Procedia, 117 (2017): 291–298. https://doi.org/10.1016/j.egypro.2017.05.134

[8]   Kriswanto and Jamari, Radial Forces Analysis and Rotational Speed Test of Radial Permanent Magnetic Bearing For Horizontal Axis Wind Turbine Applications", AIP Conference Proceedings 1725, (2016): 020034 1-10 https://doi.org/10.1063/1.4945488

[9]   Daniel DV, Tănase N, Apostol ES, Chiriţă I and Ilie C, "An overview regarding the analytical vs. numerical computation for a PMB used for FESS," 2017 10th International Symposium on Advanced Topics in Electrical Engineering (ATEE), (2017): 458-462 https://doi.org/10.1109/ATEE.2017.7905044

[10]   Teng, W., X, Ding., X. Zhang., L. Y. Liu. and Z. Ma. Multi-fault detection and failure analysis of wind turbine gearbox using complex wavelet transform. Renewable Energy 93 (2016): 591-598. https://doi.org/10.1016/j.renene.2016.03.025

[11]   Bekinal. S. I. and M. Doddamani. Friction-Free Permanent Magnet Bearings for Rotating Shafts : A Comprehensive Review. Progress In Electromagnetics Research C 104 (2020): 171–186 https://doi.org/10.2528/PIERC20060402

[12]   Parambil, L. K. Design methodology for monolithic layer radial passive magnetic bearing. Journal of Engineering Tribology (2019): 1-9. https://doi.org/10.1177/1350650118806372

[13]   Zhang, L., H. Wu., P. Li., Y. Hu. and C. Song. Design, analysis, and experiment of multiring permanent magnet bearings by means of equally distributed sequences based Monte Carlo method," Mathematical Problems in Engineering 2019 (2019): 1-18. https://doi.org/10.1155/2019/4265698

[14]   Wang R, Han T, Wang W, Xue Y, and Fu D. Fracture analysis and improvement of the main shaft of wind turbine based on finite element method. Advances in Mechanical Engineering 10 (2018): 1–9. https://doi.org/10.1177/1687814018769003

[15]   Anonymous. 2021. Ovako 34CrNiMo6 SB9205 Steel. http://www.matweb.com/search/DataSheet.aspx?MatGUID=e3376bb4f6ab4d9ba23f4b7aa7f1882a&ckck=1

[16]   Ni, Q., K. Feng., K. Wang., B. Yang. dan Y. Wang. A case study of sample entropy analysis to the fault detection of bearing in wind turbine. Case Studies in Engineering Failure Analysis 9 (2017): 99–111. https://doi.org/10.1016/j.csefa.2017.10.002

[17]   Ge, Y and Wang. K. Influence of Microalloying Element on the Microstructure and Mechanical Properties of 34CrNiMo6 Steel for Wind Turbine Main Shaft. Advance in Material Science and Engineering 2018 (2018): 1-6. https://doi.org/10.1155/2018/2672385

[18]   Huang CP, Lin X, Liu FC, Cao J, Liu FCG, and Huang WD. Effects of cooling condition on microstructure and mechanical properties in laser rapid forming of 34CrNiMo6 thin-wall component. Int J Adv Manuf Technol 82 (2016): 1269–79, https://doi.org/10.1007/s00170-015-7453-z

[19]   Branco R, Costa JD, Berto F, Kotousov A, and Antunes FV. 2020. Fatigue crack initiation behaviour of notched 34CrNiMo6 steel bars under proportional bending-torsion loading. Int J Fatigue 130, (2020): 105268 1-10. https://doi.org/10.1016/j.ijfatigue.2019.105268

[20]   Aryadi W, Kriswanto, Roziqin A and Jamari. 2021 IOP Conf. Series: Earth and Environmental Science vol 700 pp.1-7. https://doi.org/10.1088/1755-1315/700/1/012006

[21]   Roziqin A, Kriswanto and Aryadi W 2021 IOP Conf. Series: Earth and Environmental Science vol 700 pp. 1-8 https://doi.org/10.1088/1755-1315/700/1/012008

[22] Kriswanto, Supraptono, Roziqin A, Hasyim F, Saputro D D and Wijayanto B 2021 IOP Conf. Series: Earth and Environmental Science Vol. 700 pp. 1 https://doi.org/10.1088/1755-1315/700/1/012004

[23] Azizan A, Israr, H A, and Tamin M N. (2020). Effect of Fiber Misalignment on Tensile Response of Unidirectional CFRP Composite Lamina . Journal of Advanced Research in Applied Sciences and Engineering Technology, 11(1), 23–30.

[24] J. Ibrahim, M I, and Mohamed Yusoff M Z. (2020). Optimization of Interlocking Structures Made of Flax Fibre Composites to Improve Its Energy Absorption Capability. Journal of Advanced Research in Applied Sciences and Engineering Technology, 10(1), 1–17.

[25] Veritas DN. 2002. *Design of Wind Turbines*. 2 edition. Norwegia: Det Norske Veritas & Risø National Laboratory.

[26] Nasri, W. ., Djebali, . R. ., Goodarzi, M. ., Abbassi, M. A. ., & Abboudi, S. . (2021). Apple Convective Drying - Part I: Finite Elements Parametric Study for Appraising the Operating Conditions Effects. CFD Letters, 11(3), 28–41.

[27] Ramlan., Muljadi., P. Sardjono., F. Gulo., and D. Setiabudidaya. Crystal Structure and Magnetic Properties of $Nd_2Fe_{14}B$ Powder Prepared by Using High Energy Milling from Elements Metal Nd,Fe,B Powders. Journal of Physics 776 012013 (2016):1-6 https://doi.org/10.1088/1742-6596/776/1/012013

[28] Suprapedi, Sardjono P, and Muljadi. 2016. Physical and magnetic properties, microstructure of bonded magnet NdFeB prepared by using synthesis rubber. Journal of Physics: Conference Series 776 012015 (2016): 1-6 https://doi.org/10.1088/1742-6596/776/1/012015

[29] Wang, X., Zhu, K., Li, W., Xu, J., Ali, Z., and Hou, Y. $Nd_2Fe_{14}B$ hard magnetic powders: chemical synthesis and mechanism of coercivity. Journal of Magnetism and Magnetic Materials 518 (2020): 1-6. https://doi.org/10.1016/j.jmmm.2020.167384

[30] Jeong, J. H., Ma, H. X., Kim, D., Kim, C. W., Kim, I. H., Ahn, J. W. Kim DS, and Kang, Y. S.. Chemical synthesis of $Nd_2Fe_{14}B$ hard phase magnetic nanoparticles with an enhanced coercivity value: effect of CaH_2 amount on the magnetic properties. New Journal of Chemistry 40, (2016) 10181–10186*.* https://doi.org/10.1039/C6NJ02436J

[31] Krugel G, Körner W, Daniel FU, Gutfleisch O and Elsässer C. High-Throughput Screening of Rare-Earth-Lean Intermetallic 1-13-X Compounds for Good Hard-Magnetic Properties. Metals 9 (2019): 1-13. https://doi.org/10.3390/met9101096

[32] Constantinides, S., and J. D. Leon. (2017). Permanent Magnet Materials and Current Challenges Development of Magnet Materials. Arnold Magnetic Technology, Denmark.

[33] Schroeter, H. (2007). Permanent Magnets Materials and Magnet Systems. IBS Magnet, Berlin.

[34] Bekinal, S. I., T. R. Anil. and S. Jana. Analysis Of Axially Magnetized Permanent Magnet Bearing Characteristics. Progress In Electromagnetics Research B. 44 (2012): 327–343. https://doi.org/10.2528/PIERB12080910

[35] Zhang L, Wu H, Li P, Hu Y, and Song C.2019. Design, Analysis, and Experiment of Multiring Permanent Magnet Bearings by Means of Equally Distributed Sequences Based Monte Carlo Method, Mathematical Problems in Engineering 2019 (2019): 1-17. https://doi.org/10.1155/2019/4265698 z

4. Bukti konfirmasi artikel *accepted submission* (14 November 2021)

UNNES
UNIVERSITAS NEGERI SEMARANG

Kriswanto Unnes <kriswanto@mail.unnes.ac.id>

[J. Adv. Res. Fluid Mech. Therm. Sc.] Editor Decision

2 messages

Nor Azwadi <azwadi@semarakilmu.com.my>   Sun, Nov 14, 2021 at 12:02 PM
To: Kriswanto <kriswanto@mail.unnes.ac.id>

Kriswanto:

We have reached a decision regarding your submission to Journal of Advanced Research in Fluid Mechanics and Thermal Sciences, "EIC-Analysis of an Axial Permanent Magnetic Bearing for 1MW Horizontal Axis Wind Turbine ".

Our decision is to: Accept Submission

Thank you

Truly

Editor-in-chief, Journal of Advanced Research in Fluid Mechanics and Thermal Sciences

_____

Journal of Advanced Research in Fluid Mechanics and Thermal Sciences

Kriswanto Unnes <kriswanto@mail.unnes.ac.id>   Sun, Nov 14, 2021 at 10:41 PM
To: Nor Azwadi <azwadi@semarakilmu.com.my>

Thank you for the information.
[Quoted text hidden]

Konfirmasi artikel accepted di OJS SEMARAK ILMU

Notifications ×

[J. Adv. Res. Fluid Mech. Therm. Sc.] Editor Decision

2021-11-14 05:02 AM

Kriswanto:

We have reached a decision regarding your submission to Journal of Advanced Research in Fluid Mechanics and Thermal Sciences, "EIC-Analysis of an Axial Permanent Magnetic Bearing for 1MW Horizontal Axis Wind Turbine ".

Our decision is to: Accept Submission

Thank you

Truly

Editor-in-chief, Journal of Advanced Research in Fluid Mechanics and Thermal Sciences

_____
Journal of Advanced Research in Fluid Mechanics and Thermal Sciences

5. **Bukti artikel** *production (copyedited)* **dan artikel (25 April 2022)**

semarakilmu.com.my/journals/index.php/fluid_mechanics_thermal_sciences/authorDashboard/submission/9

Journal of Advanced Research in Fluid Mechanics and Thermal Sciences

← Back to Submissions

9 / **Kriswanto et al.** / Analysis of an Axial Permanent Magnetic Bearing for 1MW Horizontal Axis Wind

Library

Workflow **Publication**

Submission | Review | **Copyediting** | Production

Copyediting Discussions

Add discussion

Name	From	Last Reply	Replies	Closed
▸ Manuscript status	kriswanto 2022-04-11 12:57 AM	-	0	☐

Copyedited

Q Search

| | 921 | [9] SemarakIlmu_PMB Artikel.docx | | April 22, 2022 | Article Text |

22:57
19/06/2024

Analysis of an Axial Permanent Magnetic Bearing for 1MW Horizontal Axis Wind

Kriswanto[1,*], Rizqi Fitri Nuryanto[1], Renaldy Prasdiansyah[1], Dony Hidayat Al-Janan[1], Widya Aryadi[1], Ahmad Roziqin[1], Samsudin Anis[1], Wirawan Sumbodo[1], and Jamari[2]

[1] Department of Mechanical Engineering, Universitas Negeri Semarang, Gd E9 Kampus Sekaran Gunungpati, Semarang, Indonesia
[2] Department of Mechanical Engineering, University of Diponegoro, Jl. Prof. Sudharto Kampus UNDIP Tembalang, Semarang 50275, Indonesia

ARTICLE INFO	ABSTRACT
	One way to reduce maintenance costs while improving wind turbine efficiency is to replace mechanical bearings with permanent magnetic bearings. The permanent magnetic bearing is a free contact bearing in which the rotor is elevated from the stator by the magnet's repelling force. The purpose of this study is to analyze the variation of permanent magnet width and the gap distance between the rotor-stator magnets that can produce the magnetic axial force opposing the thrust force of 1MW horizontal axis wind turbines (HAWT). The method used in this study is a magnetic force simulation using finite element method by varying the magnet thickness, width of the gap, and displacement between the rotor-stator of the PMB model. The PMB model consists of rotor and stator magnets arranged in 3 layers with $Nd_2Fe_{14}B$ type material with a magnetic flux density of 1.45 T. Variations in thickness of the rotor and stator magnets are 0.1; 0.15, respectively; 0.2 (m), while variations in the width of the magnetic gap are 4, 5, 6 (mm). The results of the study found that the displacement that produces an axial magnetic force that can support a thrust force of 199.5kN is the lowest in the PMB model with a magnetic thickness of 0.15m with a magnetic gap of 4mm, while the highest is at a magnetic thickness of 0.1m with a magnet gap of 6mm. The greater the thickness of the PMB axial magnet design, the greater the displacement that provides zero axial magnetic forces. Further, the maximum of the magnetic axial force is rise on with increasing magnet thickness.

1. Introduction

One of the most critical components of wind turbines is the bearing. Furthermore, the wind industry has recognized main bearing failures as a major concern in terms of raising wind turbine reliability and availability, according to the European Academy of Wind Energy (EAWE) [1]. It is due to the high maintenance costs and long periods of downtime related to main bearing failures. Large-scale power plants currently apply mechanical bearings for onshore and offshore wind turbines. Nevertheless, the use of it has a limited-service life as well as capability [2]. So the effort to improve

---

the efficiency and reliability of wind turbines is to minimize friction using magnetic bearings [3]. The magnetic bearing is a bearing that utilizes refuse forces to support a rotor without physical contact [4].

Magnetic bearings have the benefit of being able to adapt to changing operating conditions and the environment. Within certain limits, the adjustment of magnetic bearing caused vibration was independent of the rotor position. Moreover, magnetic bearings can maintain rotor equilibrium positions at various loads. The rotor can rotate on its main axis and does not cause vibration on the foundation. Due to the levitation force of magnets, the vibration was significantly reduced [5]. The study of the magnetic bearing on the flywheel has the same polarity as the rotor, generating repulsive forces that keep the flywheel magnetically levitating and thereby reducing friction losses inside [6]. Nevertheless, permanent magnetic bearings (PMB) have several problems, including stability problems. Otherwise, given the long lifetime of its use then PMB is an effective solution to overcome the bearing problems [7]. The study of PMB in wind turbine prototypes to substitute mechanical bearings can enhance rotational speed and torque, therefore enhancing Horizontal Axis Wind Turbine (HAWT) performance [8]. Comparative study of axial force results of PMB between analytical approach and finite element method shows good agreement between the two [9].

The permanent magnetic bearing has been applied for rotating shafts that are used to replace conventional bearings which have high maintenance costs and friction [11]. Therefore, maintenance costs of wind turbines can be minimized by the use of permanent magnetic bearings. It is aligned with the statement that passive magnetic bearing is one of the most economical and effective methods to lift the two surfaces in relative motion that do not require active control and additional energy [12].

The study of modeling of the axial permanent magnetic bearing that comparing the theoretical simulation of the Monte Carlo method and the finite element method found that errors approximate zero and are consistent. Moreover, the experimental results are consistent with the simulation analysis [13]. The previous study [3-8] [10-12] shows the permanent magnetic bearings reduce friction, minimizes maintenance costs, can replace mechanical bearings. While none of the above literature has developed or studied the axial force of a PMB for a 1MW HAWT. The main shaft bearing of the HAWT must support both radial and axial loads (thrust forces). Furthermore, the HAWT thrust force is affected by the cut in and cut out of wind speed. The higher the wind speed, the higher the axial load on the main shaft bearing HAWT. Therefore, this paper presents to analyzes the axial magnetic force of the several thicknesses and air gaps of the permanent magnetic bearing models as the main bearing of the 1MW HAWT. Magnetic force and displacement are analyzed to find the shortest gap that can sustain the highest thrust force (at the cut out of wind speed). The main bearing locates near the gearbox, as shown in Figure 1 and indicated by number 2.
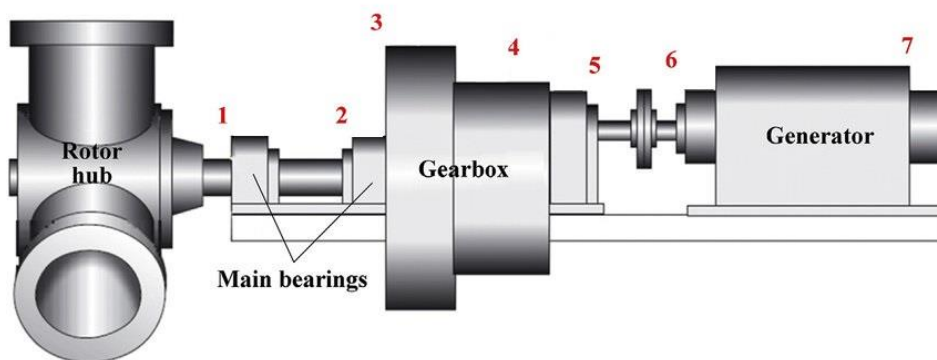

Fig. 1. Main shaft bearings [10]

2. Methodology

The main shaft of the HAWT model, made of 34CrNiMo6 steel, complies with wind turbine certification standards [14]. Furthermore, it was analyzed by finite element method and confirmed by Mohr II theory calculations to get the deflection value due to radial load. The defection will be used as the minimum air gap to prevent collisions between the rotor magnets and the stator magnets. The material properties of 34CrNiMo6 steel used in the finite element method are the density of 7800 (kg/m^3), elasticity modulus by 210 GPa, and Poisson's ratio of 0.3 [15]. The main shaft must be safe during operation to prevent damage that causes unexpected economic losses [16]. Furthermore, the 34CrNiMo6 steel has good toughness properties also the shock resistance of the material is good enough in the operating environment temperature [17]. In addition to being applied to wind turbine shafts, 34CrNiMo6 is high-strength structural steel frequently used in large-sized shaft components with complex geometry, such as aircraft propeller shafts and automobile connecting rods [18-19]. The specifications for the horizontal axis wind turbine show in Table 1.

Table 1
HAWT model specifications

Part name	Specification	Value
Rotor Blade	Number of blades	3
	Diameter (m)	54.4
	power coefficient, C_P	0.4877
	Tip Speed Ratio, TSR	2.82
	Rotor Load (N)	164150
Main shaft	Density, ρ (kg/m^3)	7800
	Diameter (m)	1.25
	Massa, m (Kg)	404.3
	Length, l (m)	4.5
	Material	34CrNiMo6
Bearing	Diameter Bore (m)	1.25
	Outer diameter (m)	2.2
	Material	$Nd_2Fe_{14}B$
	Remanent flux density, B_r (T)	1.45
Control	Cut in speed (m/s)	3.5
	Cut out speed (m/s)	15

The maximum deflection is the distance of the shaft to prevent the possibility of friction between the stator magnet and the rotor magnet. This calculation uses two methods, namely the finite element analysis method and Mohr's Theory calculation. Many uses of FEM in the structural field are to analyze stresses and displacements [20-24]. The bending moment diagram on the HAWT main shaft shows in Figure 2.
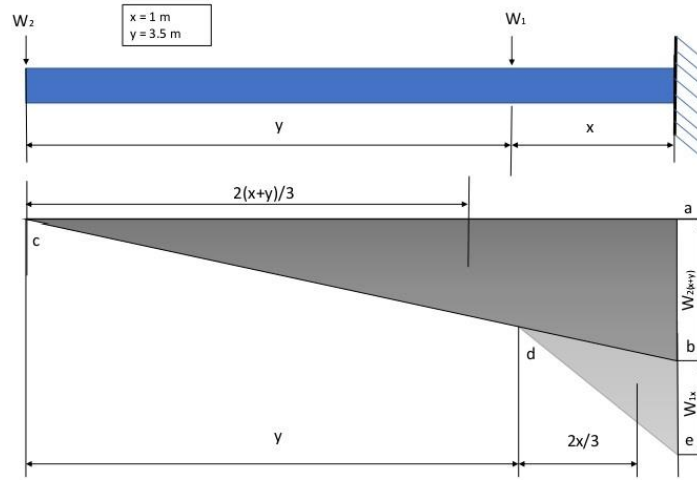
Fig. 2. Bending moment diagram of HAWT main shaft

which x (m) is the distance from the base of the shaft to the center of the magnetic load, y is the distance from the center of gravity to the end shaft (m), W_1 is the rotor magnet load (N), and W_2 is the total load from the connector hub load and the rotor load (N). Hereafter, the Eq. (1) and Eq. (2) for the deflection calculations.

$$I_P = \pi 4 \left(r_{c2}{}^4 - r_{c1}{}^4 \right) \tag{1}$$

$$\delta = \frac{1}{EI} \int_X^Y \mathrm{M} \, x \, \mathrm{d}x \tag{2}$$

where I_P is the polar inertia of the shaft, r_{c1} is the inner radius of the shaft cylinder, r_{c2} is the outer radius of the shaft cylinder, E modulus of elasticity of 34CrNiMo6, M is an area of the bending moment diagram, x is the distance of the load to the base of the shaft, and δ is the maximum deflection of the shaft. The data for each variable is present in Table 2.

Table 2
Properties on HAWT main shaft

x [m]	y[m]	W_1 [N]	W_2 [N]	r_{c1} [m]	r_{c2} [m]	E [GPa]
1	3.5	17,283	164,150	0.225	0.625	210

The location of the axial PMB on the HAWT main shaft is shown in Figure 3, wherein the position is closer to the gearbox. The free-body diagram of the force and moment on the main shaft see in Figure 4. The thrust force received by the rotor from the wind calculate using Eq. (4).
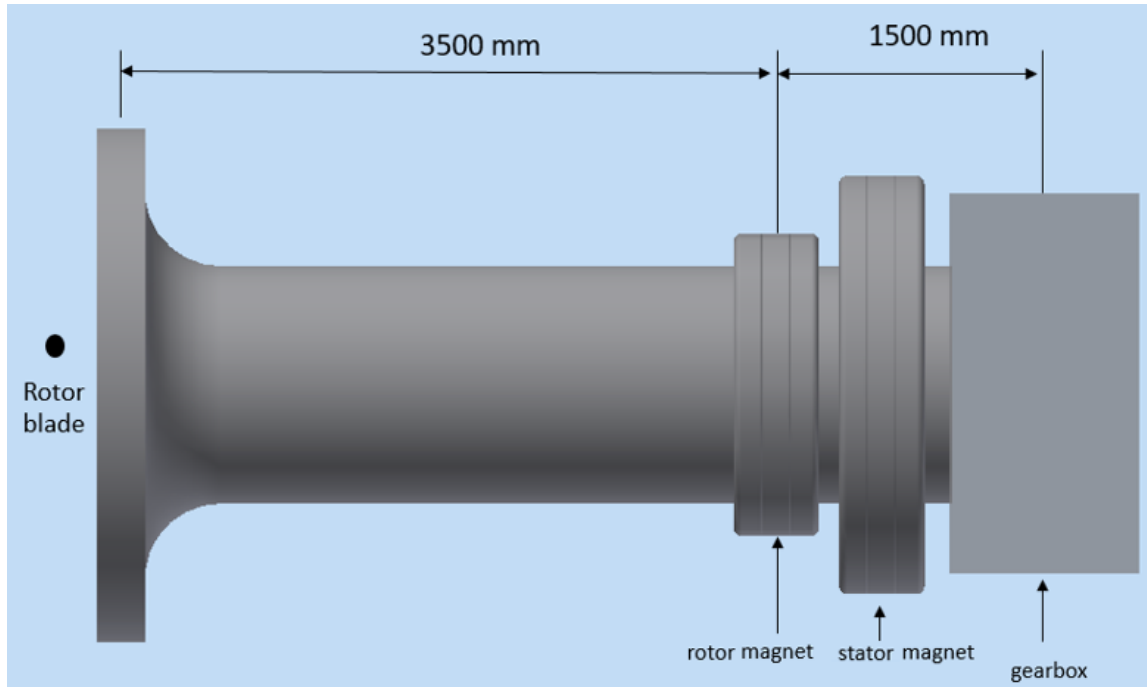
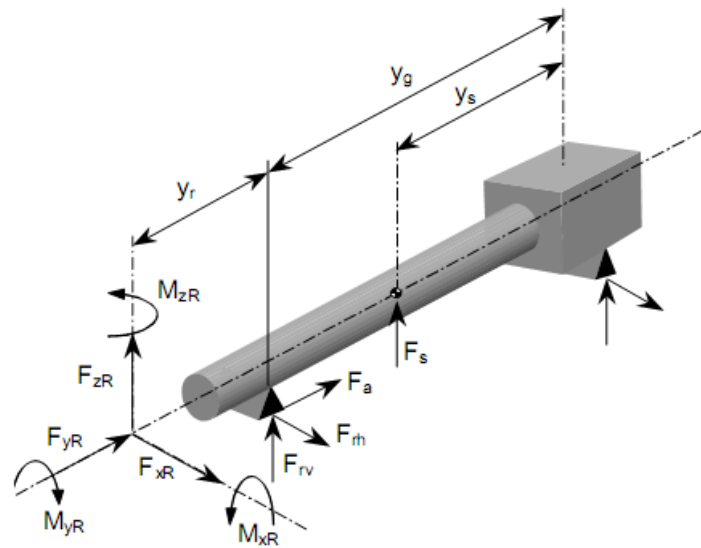**Fig. 3.** Location of axial PMB on the HAWT main shaft

Fig. 4. Forces and moments on the HAWT main shaft [25]

$$A = \pi \, r2 \tag{3}$$

$$F_{yR} = \frac{1}{2} \rho A \left(v_1^2 - v_2^2 \right) \tag{4}$$

The magnetic force simulation in this study uses the finite element method assisted of COMSOL by integrating vector Eq. (5). COMSOL software is a powerful modeling and simulation tool for engineering and industrial applications combining several physics connections [26]. The axial force of the PMB model was simulation by displacement distance between the rotor magnet against the stator.

$$f = n.T = -\frac{1}{2} n(H.B) + (n.H)B^T \tag{5}$$

where f is the magnetic force (n), n is the external normal vector, T is the tensor stress Maxwell, H is the magnetic field/ coercivity, B is the magnetic flux density (T).

The magnetic model uses the relationship between the density of the magnetic lines force and the magnetic field, which is expressed by Eq. (6).

$$B = \mu_r \mu_0 H \tag{6}$$

where μ_r is the relative permeability and μ_0 is the absolute magnetic permeability.

Magnetic field using Ampere's law model, with the stationary magnetic field Eq. (7).

$$B = \bar{V} A' \tag{7}$$

$$\mu_0{}^{-1} \mu_r{}^{-1} \bar{V} A' = J \tag{8}$$

where $\bar{V}$ is the vector operators, A' is the Magnetic potential vector, and J is the magnetization residual or magnetism induction density. Boundary conditions using the Eq. (9).

$$n_1 A' = 0 \tag{9}$$

The magnetic field was the model using a magnetic field interface model. Ampere's law used to include magnetic field physics into all free air domains. The infinite element domain uses to simulate the large region of free space surrounding the magnets. The material for all free domains is air. The free triangular mesh generated in the simulation is both the computational domain and the magnets. In this study, the magnet material made from $Nd_2Fe_{14}B$, which the magnet is composed of a mixture of neodymium (Nd), iron powder (Fe), and boron powders (B) using the high compression molding method [27]. The $Nd_2Fe_{14}B$ is a kind of hard magnet with excellent magnetic characteristics, possesses the highest values of maximum energy product (BH) max and coercivity [28-30]. In addition, $Nd_2Fe_{14}B$ is the strongest permanent magnet because maximum energy reaches more than $400kJ/m^3$ [31-33]. Figure 5 show the HAWT main shaft design, all dimensional units of mm. The diameter of the HAWT main shaft is a limitation in determining the inner diameter of the PMB rotor magnet.
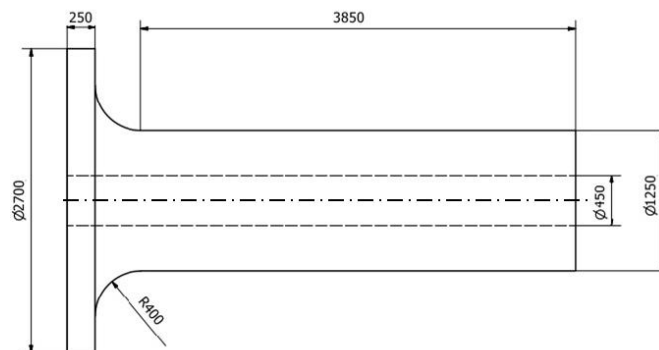

Fig. 5. HAWT main shaft design

As illustrated in Figure 6, the PMB axial configuration design includes three magnets on the rotor magnet B and the stator magnet A, which has a magnetic force density direction like in Figure. The rotor magnet is an inner magnet with an outer diameter smaller than the stator magnet's inner diameter, resulting in a gap. Placement of the rotor magnet against the stator, *LZ0* must be in a

condition where there is no axial magnetic force interaction between the two (F_z=0N). This setting is a condition when the wind turbine rotor does not receive thrust force from the wind. Meanwhile, the maximum thrust force or at the cut-out wind speed must restrain by the PMB thrust force with the smallest possible displacement distance (ΔZ).
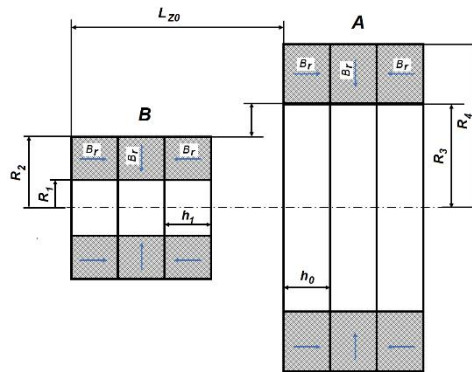

Fig. 6. Design of axial PMB configuration

The design specifications of the axial PMB model are presented in Table 3, wherein the model uses a configuration of concentric ring permanent magnets which have different dimensions and have opposite directions of magnetic force density (Br). Furthermore, the axial PMB in the present study functions as the axial main shaft bearing of HAWT.

Table 3
PMB model specifications

	Outer magnet, A	Inner magnet, B
Inner Radius (m)	R_3 = 0.805; 0.806; 0.8067	R_1 = 0.625
Outer Radius (m)	R_4 = 1.1	R_2 = 0.8
Thickness (m)	h_0 = 0.1; 0.15; 0.2	h_1 = 0.1; 0.15; 0.2
Magnetic Flux Density, Br (T)	1.45	1.45

3. Results
3.1 Thrust Force on The HAWT Main Shaft

The Thrust force (F_{yR}) of the HAWT main shaft is calculated by Eq. (3), which A of 2323.098 m^2 and ρ is the air density assumed is 1.293 kg/m^3. The thrust force results on the HAWT main shaft are shown in Figure 7.
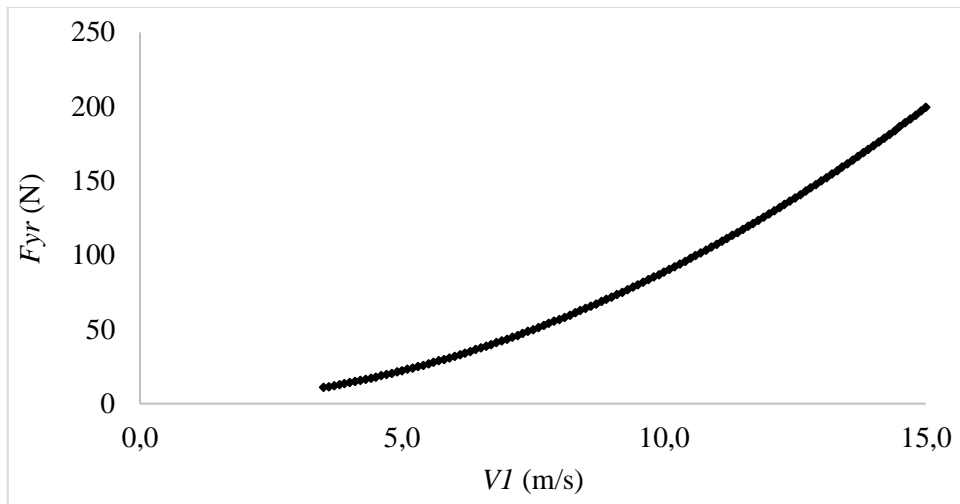
Fig. 7. Graph of the thrust force on the HAWT main shaft vs windspeed

The minimum thrust force is 10862.22 N generated at a wind speed of 3.5 m/s at the cut-in of HAWT, while the maximum is 199.5kN generated at a wind speed of 15 m/s, namely at a HAWT cut-out. The higher the wind speed, the higher the thrust force. According to Figure 7, the HAWT main shaft bearing must sustain an thrust force of 199.5 kN.

3.2 Maximum Deflection on The Main Shaft Of HAWT

The maximum deflection is analyzed to determine the minimum gap between the rotor magnets and the stator not to touch later. The results obtained from the finite element method (FEM) use COMSOL will then compare with mathematical of the Mohr II theoretical equation. The results of the maximum deflection analysis show in Figure 8.
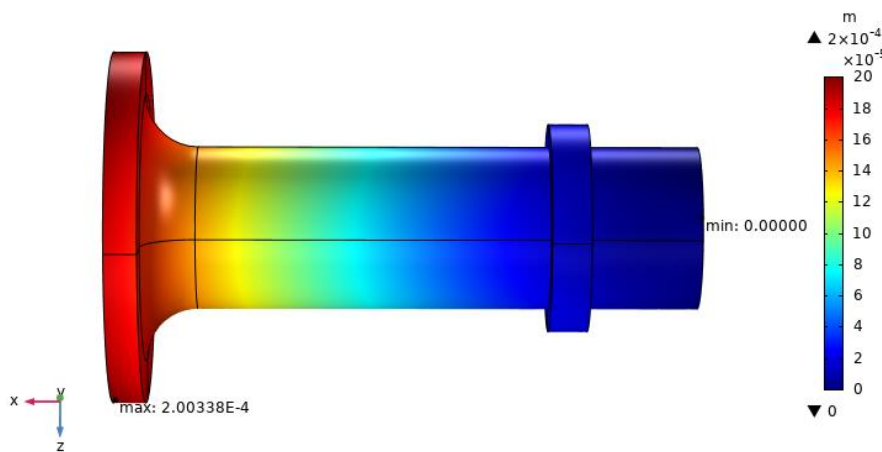

Fig. 8. Maximum deflection of HAWT main shaft use FEM

The maximum deflection of the modeling approximates analytic calculations using Mohr II theory (see Table 4). Moreover, the discrepancy between the two methods above has 0.015 %, which indicates that the FEM agrees with the analytic.

Table 4
Model Validation with Mohr II theory

	FEM	Analytic	Variation (%)
Maximum Deflection (mm)	0.20033	0.20036	0.015

3.3 PMB Model Validation

Figure 9 is a plot of axial force versus displacement generated from the modeling, where the axial force Fz is 126.12 N, is the rotor magnet experiences an of the stator as far as 6mm towards the positive axial direction dZ. This also applies to the displacement that leads to negative axial where at dZ at a distance of -6mm an axial force Fz equal to -126.12 N is produced.
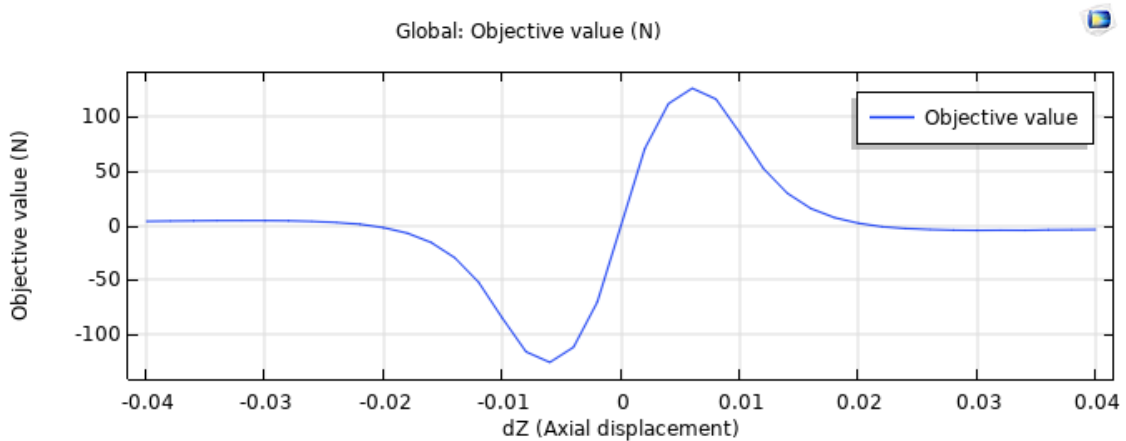

Fig. 9. Plot of the magnetic axial force of the modelling

The maximal axial force obtained through modeling is 126.12N, whereas the Bekinal mathematical model yields 126.59N (see Table 5). The discrepancy between the results of the two methods is 0.37%, which indicates that the modeling method is declared valid.

Table 5
Validation of the axial force with Bekinal model

	Modeling	Bekinal model [34]	Variation (%)
Axial Force (N)	126.12	126.59	0.37

3.4 Axial Force Modeling Of 0.1 M Magnet Thickness of the PMB

The axial PMB design is depicted in Figure 6, then the parameters provided in Table 1 have values of h_0-h_1 indicate a magnet thickness of 0.1 m. The variation in this configuration lies in the width of the magnetic gap with R_3 values are 0.805, 0.806, 0.807 (m), so that the magnetic gap c becomes 4 mm, 5 mm, and 6 mm. The maximum magnetic flux density of 1.45T (see Figure 10(a)) at 0.1 m thickness variation and 4mm gap as shown in the red area concentrated in the center of the magnet both on the rotor and stator. Figure 10(b) depicts the axial force towards displacement with dZ – 0.38 m to 0.38 m.
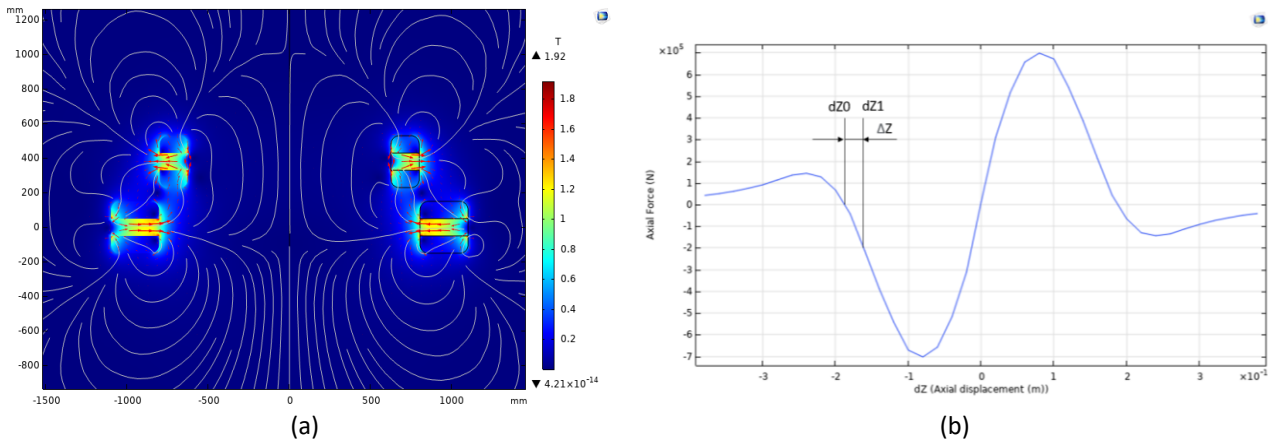
(a) (b)

Fig. 10. Plot of the axial PMB h_0 h_1 0.1 m, c 4mm, (a) magnetic flux density (b) axial force-displacement range *dZ* -0.38 to 0.38 m

Figure 11 is a plot of the axial force versus displacement generated in the axial PMB simulation with a magnetic thickness of 0.1 m which the width is varied for the magnetic gap "c" (4mm; 5mm; and 6mm) and for the distance set at *dZ* −190mm to -140mm. The rotor-stator distance that produces 0N (*LZ0*) magnetic axial force is 187mm. The measurement of *ΔZ* starts from the displacement point of the rotor-stator at an axial force of 0N (*dZ0*) to the location (*dZ1*) wherein F_Z 199.5 kN is produced. The thrust force on the HAWT main shaft, which is 199.5 kN, can be supported by axial PMB at *c* 4mm with displacement *ΔZ* 26mm, *c* 5mm with *ΔZ* 27mm, and *c* 6mm, the distance *ΔZ* is 28mm. Based on the simulation results, the minimum displacement against the thrust force is found at c 4mm. Furthermore, this configuration can support the axial load on the HAWT main shaft with a *ΔZ* value of 2.6mm.
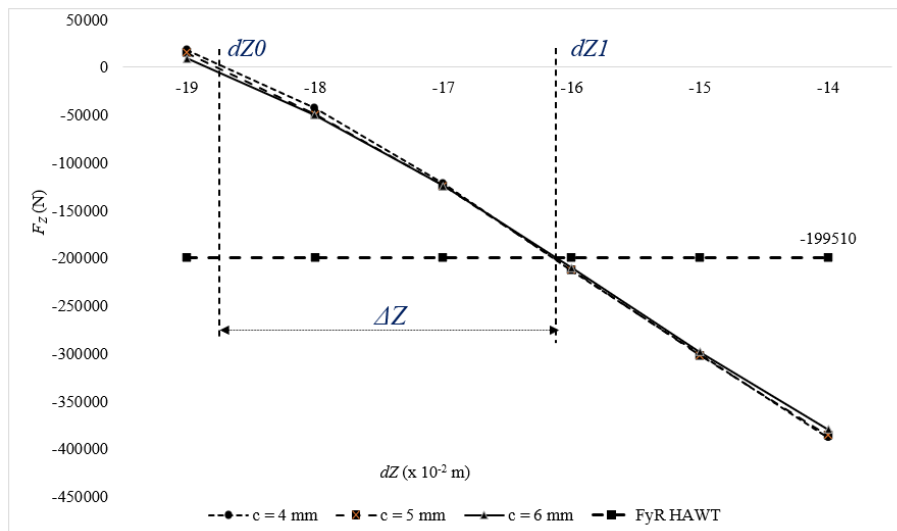

Fig. 11. The plot of the axial force-displacement of axial PMB, with h 0.1 m

3.5 Axial Force Modeling Of 0.15 M Magnet Thickness of the PMB

The axial PMB design uses the parameters provided in Table 1 have values of h0-h1 indicate a magnet thickness of 0.15 m. The difference in this configuration magnetic gap c values of 4mm, 5mm, and 6mm. Figure 12(a) shows the maximum magnetic flux density of 1.45T at 0.15 m thickness variation and 4mm gap, which is centered in the magnet's center on both the rotor and stator. Figure 12(b) shows the axial force-displacement which $dZ - 0.38$ m to 0.38 m.
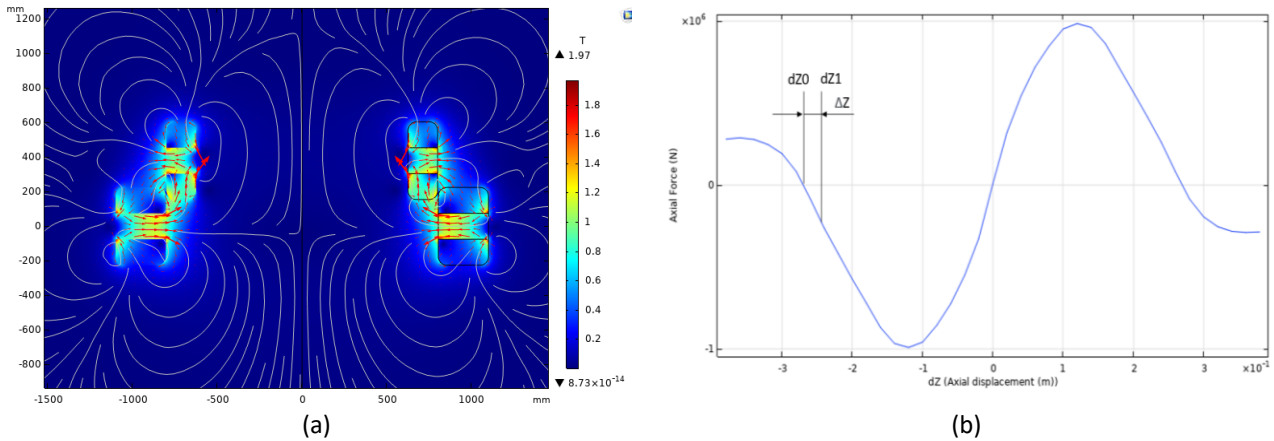

Fig. 12. Plot of the axial PMB h_0 h_1 0.15 m, c 4mm, (a) magnetic flux density (b) axial force-displacement range dZ -0.38 to 0.38 m

Figure 13 shows a plot of the axial force against displacement created in the axial PMB simulation with a magnetic thickness of 0.15 m and a magnetic gap "c" (4mm; 5mm; 6mm) and a distance set at $dZ - 270$mm to -220mm. The rotor-stator distance required to generate ($LZ0$) 0 N magnetic axial force is 270mm.The thrust force of 199.5 kN on the HAWT main shaft may be sustained by axial PMB at c 4mm with displacement ΔZ 22mm, c 5mm with displacement ΔZ 22mm, and c 6mm with distance ΔZ 23mm. According to the results, the minimum displacement sustain the thrust force is discovered at c 4mm. Furthermore, with a ΔZ value of 22mm, this arrangement can sustain the axial load on the HAWT main shaft. The simulation results of the axial magnetic force at 0.15m thickness of the magnet is similar to 0.1m thickness configuration, wherein the air gap (c) the smaller the displacement smaller too.
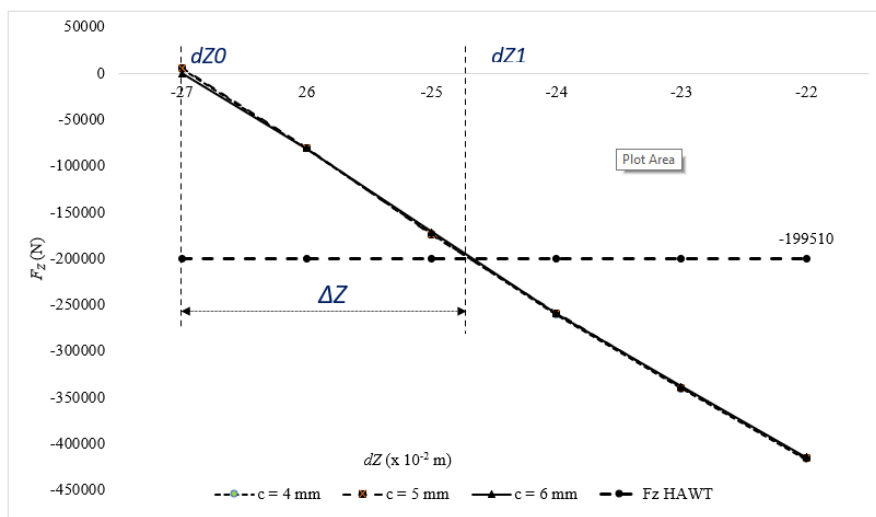

Fig. 13. Plot of the axial force -displacement of axial PMB, with h 0.15 m

3.6 Axial Force Modeling Of 0.2 M Magnet Thickness of the PMB

The axial PMB design proposes the specifications shown in Table 1, with h_0-h_1 indicating a magnet thickness of 0.2m. The magnetic gap c values of 4mm, 5mm, and 6mm differ in this arrangement. Figure 14(a) depicts the maximum magnetic flux density of 1.45T in the central magnetic region of the rotor and stator, for 0.2 m thickness variation and 4mm gap of the axial PMB Design. Figure 14(b) depicts the axial force-displacement relationship with dZ – 0.38 m to 0.38 m.
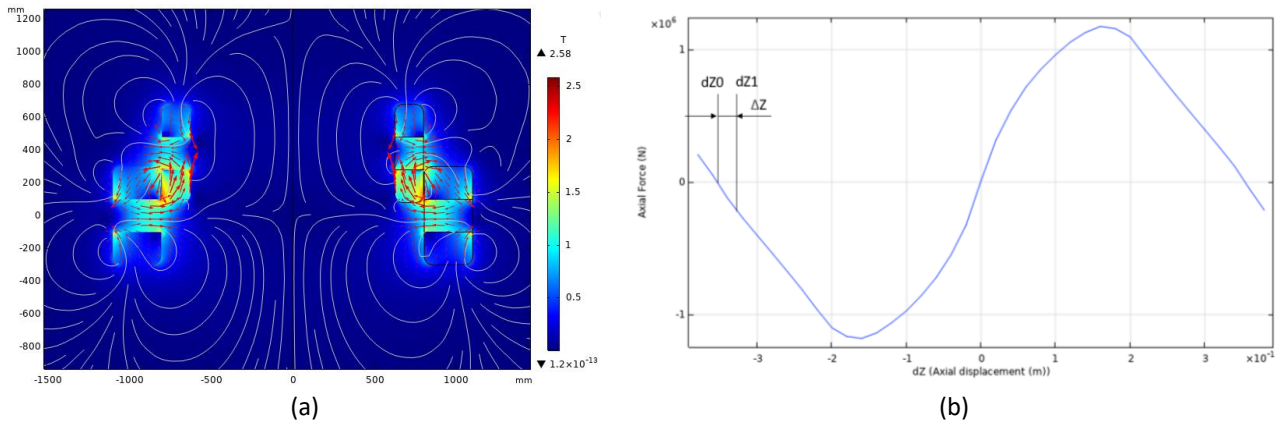

Fig. 14. Plot of the axial PMB h_0 h_1 0.2 m, c 4 mm, (a) magnetic flux density (b) axial force-displacement range dZ -0.38 to 0.38 m

Figure 15 displays the plot of axial force versus displacement of the axial PMB simulation with a magnetic thickness of 0.2 m, a magnetic gap "c" (4mm; 5mm; 6mm), and a distance set dZ –360mm to -310mm. The distance between the rotor and the stator generates 0N magnetic axial force ($LZ0$) is 354 mm. The HAWT thrust force of 199.5 kN was sustained by axial PMB at c 4mm with displacement ΔZ 25mm, while at c 5 and 6mm, the displacement ΔZ was 26mm. The simulation results show that the thicker the PMB axial magnet, the greater the axial magnetic force.
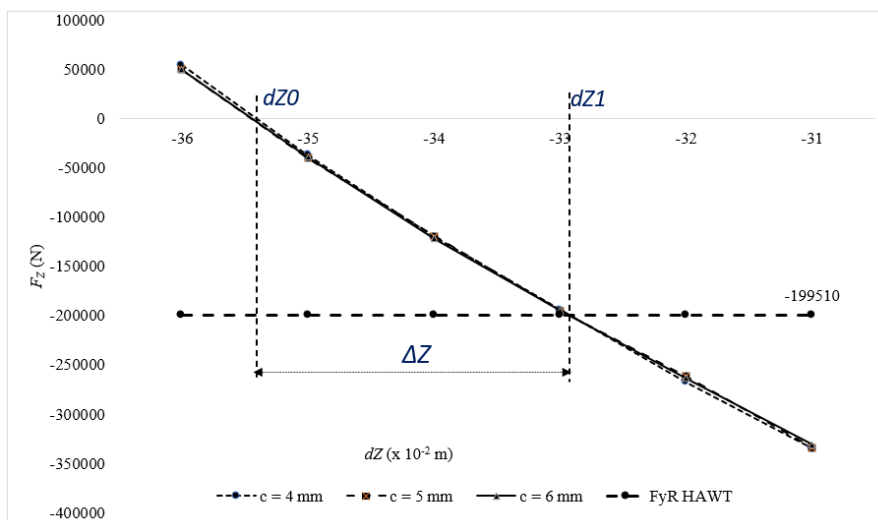
Fig. 15. Plot of the axial force -displacement of axial PMB, with h 0.2 m

The Magnetic axial force (F_z) from axial displacement (dZ) in the PMB axial design varied with the magnetic gap and magnetic thickness simulated using the finite element method. The magnetic thrust force must meet 199.5kN and the lowest displacement (ΔZ) in each configuration are limitations into consideration in selecting the PMB axial for the main shaft of the HAWT. Therefore,

the axial PMB with magnet thickness, h_0-h_1 of 0.15m, air gap of 4mm produces F_z value 199.5kN, with a minimum ΔZ value 22mm, which is the optimal configuration to obtain the lowest displacement as the HAWT axial bearing. Figure 15 depicts the smallest ΔZ displacement (22mm) in h1.5c4 and h1.5c5 variants, which are PMB axial designs with a thickness of 0.15m and a magnetic gap between the rotor and stator of 4 mm and 5 mm, respectively. Although ΔZ 22mm is the smallest, the flexibility range is still too wide to be utilized as a single substitute for HAWT's mechanical thrust bearing.

Figure 16 depicts the *LZ0* distance of 187mm on the Axial PMB 0.1m magnet thickness for the three magnetic gap changes (4,5,6mm), 270mm distance at 0.15m thickness, and 354mm distance at 0.2m thickness. The 0.1m magnet thickness has the lowest *LZ0* value. This demonstrates that the greater the thickness of the PMB axial magnet design, the greater the displacement that provides zero axial magnetic force, but is unaffected by changes in the magnetic gap (c). The rise in displacement value is proportional to the axial magnetic force produced, which increases with the size of the magnet's thickness (see Figure 17). However, there is small decrease produce in the axial magnetic force wherein the size of the magnetic gap (c) gets large. This result is similar to studies in that a smaller magnetic gap width will produce a higher magnetic force [7,35]. The effect of axial magnetic force fluctuation from magnetic gap variation is insignificant, with a difference of 3.16 % for axial PMB with a thickness of 0.1m, a difference of 2 % for a magnet thickness of 0.15m, and a difference of 1.69% for a magnet thickness of 0.2m.
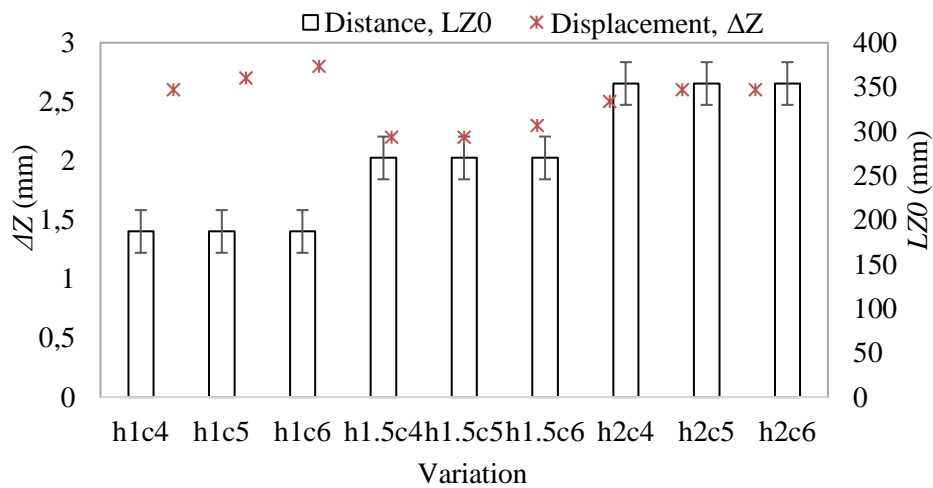

Fig. 16. Displacement ΔZ and distance *LZ0* of the axial PMB variations
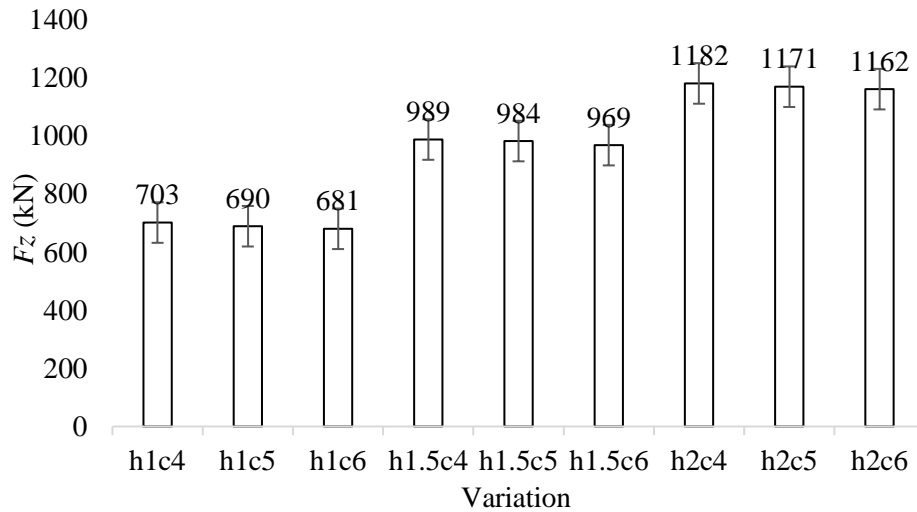
Fig. 17. The maximum of magnetic of the axial PMB variations

4. Conclusions

The permanent magnetic bearing as an axial bearing of the main shaft HAWT was designed to generate the magnetic force that resists the thrust forces from wind imposed on the rotor blades. The PMB model consists of rotor and stator magnets arranged in 3 layers that vary in thickness and width of the gap has been simulated base on the displacement of the rotor magnet against the stator. The PMB model with a thickness of 0.15m and a gap of 4mm has the shortest displacement, ΔZ (22mm) that produces a minimum axial magnetic force of 199.5 kN compared to other variations. However, this displacement has a considerable distance, so it is not feasible to use it as a single replacement for HAWT's axial bearing unless combined with the HAWT shaft main bearing close to the rotor. It is also feasible to decrease axial displacement by increasing the number of PMB axial models in one main axis of the HAWT. Analysis shows that the greater the magnet thickness of the PMB, the greater the magnetic axial force and the displacement that provides zero axial magnetic force. Furthermore, increasing the size of the rotor magnet gap towards the stator decreases the magnetic force even though small. The insignificant decrease in the value of the axial force is due to the variation of small gap magnet width. The highest decrease was found of the PMB model with a 0.1m thick magnet, where the magnetic force generated at a 4mm magnet gap compared to a 6mm magnetic gap decreased by 3.16%.

References

[1] Encalada-Dávila, Ángel, Bryan Puruncajas, Christian Tutivén, and Yolanda Vidal. "Wind Turbine Main Bearing Fault Prognosis Based Solely on SCADA Data." *Sensors* 21, no. 6 (2021): 2228. https://doi.org/10.3390/s21062228
[2] Tazi, Nacef, Eric Châtelet, and Youcef Bouzidi. "Wear analysis of wind turbine bearings." *International Journal of Renewable Energy Research (IJRER)* 7, no. 4 (2017): 2120-2129.
[3] Fekry, Mohamed, Abdelfatah M. Mohamed, Mohamed Fanni, and Shigeo Yoshida. "A comprehensive performance assessment of the integration of magnetic bearings with horizontal axis wind turbine." *Mathematics and Computers in Simulation* 156 (2019): 1-39.https://doi.org/10.1016/j.matcom.2018.06.011
[4] Zhang, Weiyu, and Huangqiu Zhu. "Radial magnetic bearings: An overview." *Results in physics* 7 (2017): 3756-3766. https://doi.org/10.1016/j.rinp.2017.08.043
[5] Jin, Chaowu, Yuanping Xu, Jin Zhou, and Changli Cheng. "Active Magnetic Bearings Stiffness and Damping Identification from Frequency Characteristics of Control System." *Shock and Vibration* 2016 (2016): 1-8. https://doi.org/10.1155/2016/1067506
[6] Alami, Abdul Hai. "Introduction to mechanical energy storage*." Reference Modeule in Earth Systems and Environmental Sciences.* Elsevier. 2021 https://doi.org/10.1016/B978-0-12-819723-3.00080-9

[7]   Micha, Premkumar T., Thangaraj Mohan, and Seralathan Sivamani. "Design and analysis of a permanent magnetic bearing for vertical axis small wind turbine." *Energy Procedia* 117 (2017): 291-298. https://doi.org/10.1016/j.egypro.2017.05.134

[8]   Kriswanto, and Jamari. "Radial forces analysis and rotational speed test of radial permanent magnetic bearing for horizontal axis wind turbine applications." In *AIP Conference Proceedings*, vol. 1725, no. 1, p. 020034. AIP Publishing LLC, 2016. https://doi.org/10.1063/1.4945488

[9]   Daniel, Dan V., Nicolae Tănase, E. S. Apostol, Ionel Chiriţă, and Cristinel Ilie. "An overview regarding the analytical vs. numerical computation for a PMB used for FESS." In *2017 10th International Symposium on Advanced Topics in Electrical Engineering (ATEE)*, pp. 458-462. IEEE, 2017. https://doi.org/10.1109/ATEE.2017.7905044

[10]   Teng, Wei, Xian Ding, Xiaolong Zhang, Yibing Liu, and Zhiyong Ma. "Multi-fault detection and failure analysis of wind turbine gearbox using complex wavelet transform." *Renewable Energy* 93 (2016): 591-598. https://doi.org/10.1016/j.renene.2016.03.025

[11]   Bekinal, Siddappa Iranna, and Mrityunjay Doddamani. "Friction-free permanent magnet bearings for rotating shafts: A comprehensive review." *Progress In Electromagnetics Research C* 104 (2020): 171-186. https://doi.org/10.2528/PIERC20060402

[12]   Parambil, Lijesh K. "Design methodology for monolithic layer radial passive magnetic bearing." *Proceedings of the Institution of Mechanical Engineers, Part J: Journal of Engineering Tribology*, (2019): 1-9. https://doi.org/10.1177/1350650118806372

[13]   Zhang, Li, Huachun Wu, Peng Li, Yefa Hu, and Chunsheng Song. "Design, Analysis, and Experiment of Multiring Permanent Magnet Bearings by Means of Equally Distributed Sequences Based Monte Carlo Method." *Mathematical Problems in Engineering* 2019 (2019): 1-17. https://doi.org/10.1155/2019/4265698

[14]   Wang, Ruiming, Tian Han, Wenrui Wang, Yang Xue, and Deyi Fu. "Fracture analysis and improvement of the main shaft of wind turbine based on finite element method." *Advances in Mechanical Engineering* 10, no. 4 (2018): 1–9. https://doi.org/10.1177/1687814018769003

[15]   Anonymous. 2021. Ovako 34CrNiMo6 SB9205 Steel. http://www.matweb.com/search/DataSheet.aspx?MatGUID=e3376bb4f6ab4d9ba23f4b7aa7f1882a&ckck=1

[16]   Ni, Qing, Ke Feng, Kesheng Wang, Binyuan Yang, and Yu Wang. "A case study of sample entropy analysis to the fault detection of bearing in wind turbine." *Case studies in engineering failure analysis* 9 (2017): 99-111. https://doi.org/10.1016/j.csefa.2017.10.002

[17]   Ge, Yanming, and Kehong Wang. "Influence of Microalloying Element on the Microstructure and Mechanical Properties of 34CrNiMo6 Steel for Wind Turbine Main Shaft." *Advances in Materials Science and Engineering* 2018 (2018): 1-6. https://doi.org/10.1155/2018/2672385

[18]   Chunping, Huang, Lin Xin, Liu Fencheng, Cao Jun, Liu Fenggang, and Huang Weidong. "Effects of cooling condition on microstructure and mechanical properties in laser rapid forming of 34CrNiMo6 thin-wall component." *The International Journal of Advanced Manufacturing Technology* 82, no. 5-8 (2016): 1269-1279. https://doi.org/10.1007/s00170-015-7453-z

[19]   Branco, R., J. D. Costa, F. Berto, A. Kotousov, and F. V. Antunes. "Fatigue crack initiation behaviour of notched 34CrNiMo6 steel bars under proportional bending-torsion loading." *International Journal of Fatigue* 130 (2020): 105268. https://doi.org/10.1016/j.ijfatigue.2019.105268

[20]   Aryadi, W., A. Roziqin, and J. Jamari. "Static Structural Analysis of the Sports Utility Vehicles Patriot Chassis." In *IOP Conference Series: Earth and Environmental Science*, vol. 700, no. 1, p. 012006. IOP Publishing, 2021. https://doi.org/10.1088/1755-1315/700/1/012006

[21]   Roziqin, Ahmad, and W. Aryadi. "Finite element analysis of village car pickup ladder frame chassis-a case study." In *IOP Conference Series: Earth and Environmental Science*, vol. 700, no. 1, p. 012008. IOP Publishing, 2021. https://doi.org/10.1088/1755-1315/700/1/012008

[22]   Roziqin, A., F. Hasyim, D. D. Saputro, and B. Wijayanto. "Static Structural Analysis and Determination of Low-Cost Component Sizes of The Paper Pulper Machines." In *IOP Conference Series: Earth and Environmental Science*, vol. 700, no. 1, p. 012004. IOP Publishing, 2021. https://doi.org/10.1088/1755-1315/700/1/012004

[23]   Azizan, Azisyahirah, Haris Ahmad Israr, and Mohd Nasir Tamin. "Effect of Fiber Misalignment on Tensile Response of Unidirectional CFRP Composite Lamina." *Journal of Advanced Research in Applied Sciences and Engineering Technology* 11, no. 1 (2018): 23-30.

[24]   Ibrahim, Mohamed Ibrahim J., and Mohd Zuhri Mohamed Yusoff. "Optimization of interlocking structures made of flax fibre composites to improve its energy absorption capability." *Journal of Advanced Research in Applied Sciences and Engineering Technology* 10, no. 1 (2018): 1-17.

[25]   Veritas, Norske. *Guidelines for design of wind turbines*. Det Norske Veritas: Wind Energy Department, Risₐ National Laboratory, 2002.

[26]   Nasri, Wiem, Ridha Djebali, Marjan Goodarzi, Mohamed Ammar Abbassi, and Said Abboudi. "Apple convective

drying-Part I: Finite elements parametric study for appraising the operating conditions effects." *CFD Letters* 11, no. 3 (2019): 28-41.

[27]   Sardjono, P., F. Gulo, and D. Setiabudidaya. "Crystal structure and magnetic properties of Nd2Fe14B powder prepared by using high energy milling from elements metal Nd, Fe, B powders." In *Journal of Physics: Conference Series*, vol. 776, no. 1, p. 012013. IOP Publishing, 2016. https://doi.org/10.1088/1742-6596/776/1/012013

[28]   Sardjono, P. "Physical and magnetic properties, microstructure of bonded magnet NdFeB prepared by using synthesis rubber." In *Journal of Physics: Conference Series*, vol. 776, no. 1, p. 012015. IOP Publishing, 2016. https://doi.org/10.1088/1742-6596/776/1/012015

[29]   Wang, Xiaobai, Kai Zhu, Wei Li, Junjie Xu, Zeeshan Ali, and Yanglong Hou. "Nd2Fe14B hard magnetic powders: Chemical synthesis and mechanism of coercivity." *Journal of Magnetism and Magnetic Materials* 518 (2021): 167384. https://doi.org/10.1016/j.jmmm.2020.167384

[30]   Jeong, Ji Hun, Hao Xuan Ma, Doyun Kim, Chang Woo Kim, In Ho Kim, Jae Woo Ahn, Dong Soo Kim, and Young Soo Kang. "Chemical synthesis of Nd 2 Fe 14 B hard phase magnetic nanoparticles with an enhanced coercivity value: effect of CaH 2 amount on the magnetic properties." *New Journal of Chemistry* 40, no. 12 (2016): 10181-10186. https://doi.org/10.1039/C6NJ02436J

[31]   Krugel, Georg, Wolfgang Körner, Daniel F. Urban, Oliver Gutfleisch, and Christian Elsässer. "High-throughput screening of rare-earth-lean intermetallic 1-13-x compounds for good hard-magnetic properties." *Metals* 9, no. 10 (2019): 1096. https://doi.org/10.3390/met9101096

[32]   Constantinides, Steve, and John De Leon. "Permanent Magnet Materials and Current Challenges Development of Magnet Materials." *Arnold Magnetic Technology, Denmark*. 2017.

[33]   Schroeter, Hagen. "Permanent Magnets Materials and Magnet Systems." *IBS Magnet, Berlin.* 2007.

[34]   Bekinal, Siddappa Iranna, Anil Rao Tumkur Ramakrishna, and Soumendu Jana. "Analysis of axially magnetized permanent magnet bearing characteristics." *Progress In Electromagnetics Research* 44 (2012): 327-343. https://doi.org/10.2528/PIERB12080910

[35]   Zhang, Li, Huachun Wu, Peng Li, Yefa Hu, and Chunsheng Song. "Design, Analysis, and Experiment of Multiring Permanent Magnet Bearings by Means of Equally Distributed Sequences Based Monte Carlo Method." *Mathematical Problems in Engineering* 2019 (2019): 1-17. https://doi.org/10.1155/2019/4265698

6.Konfirmasi publish (24 Mei 2022)

Kriswanto Unnes <kriswanto@mail.unnes.ac.id>

Congratulations, your paper has been published!

1 message

Nor Azwadi <azwadi@akademiabaru.com>   Tue, May 24, 2022 at 9:02 AM
To: kriswanto@mail.unnes.ac.id, rizqi_fitri@mail.unnes.ac.id, renaldyprasd@students.unnes.ac.id,
aljanan@mail.unnes.ac.id, widyaaryadi@mail.unnes.ac.id, ar_unnes@mail.unnes.ac.id,
samsudin_anis@mail.unnes.ac.id, wirawansumbodo@mail.unnes.ac.id

Congratulations, your paper has been published!

Dear Kriswanto, Rizqi Fitri Naryanto, Renaldy Prasdiansyah, Dony Hidayat Al-Janan, Widya Aryadi, Ahmad Roziqin, Samsudin Anis, Wirawan Sumbodo, Jamari,

Your work has now been published in the   Journal of Advanced Research in Fluid Mechanics and Thermal Sciences 94, no. 1.
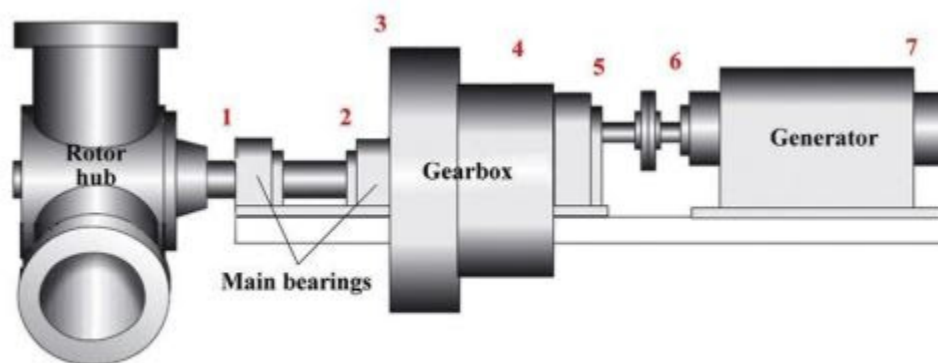

Fig. 1. Main shaft bearings [10]

Analysis of an Axial Permanent Magnetic Bearing for 1MW Horizontal Axis Wind

It's the final version of your work and can be cited, downloaded and shared.

Kriswanto, Rizqi Fitri Naryanto, Renaldy Prasdiansyah, Dony Hidayat Al-Janan, Widya Aryadi, Ahmad Roziqin, Samsudin Anis, Wirawan Sumbodo, & Jamari. (2022). Analysis of an Axial Permanent Magnetic Bearing for 1MW Horizontal Axis Wind. Journal of Advanced Research in Fluid Mechanics and Thermal Sciences, 94(1), 172–187. https://doi.org/10.37934/arfmts.94.1.172187

Promote your works to boost your citation count. You may consider the following techniques:
•   Use social media. Provide links to your papers on social media
    (e.g., Facebook, Twitter, Academia.edu, ResearchGate, Mendeley) and your university profile page.
•   Talk to other researchers about your paper, and email copies of your paper to researchers who may be interested. Create a blog or a website dedicated to your research and share it.
•   Cite your own past papers as appropriate to increase visibility of your published papers.

Thank you again for publishing with us. We wish you the best success with your research.

Kind regards

_____

INTERNATIONAL CONFERENCE ON COMPUTATIONAL HEAT TRANSFER AND FLUID MECHANICS

30 - 31st July 2022

7. Konfirmasi available in SCOPUS (14 Juni 2022)

![UNNES - Universitas Negeri Semarang logo]

Kriswanto Unnes <kriswanto@mail.unnes.ac.id>

Congratulations, your paper is now available in SCOPUS!
1 message

Nor Azwadi <azwadi@akademiabaru.com>   Tue, Jun 14, 2022 at 9:00 AM
To: kriswanto@mail.unnes.ac.id, rizqi_fitri@mail.unnes.ac.id, renaldyprasd@students.unnes.ac.id, aljanan@mail.unnes.ac.id,
widyaaryadi@mail.unnes.ac.id, ar_unnes@mail.unnes.ac.id, samsudin_anis@mail.unnes.ac.id, wirawansumbodo@mail.unnes.ac.id,
j.jamari@gmail.com

Congratulations, your paper is now available in SCOPUS!

Dear Kriswanto, Rizqi Fitri Naryanto, Renaldy Prasdiansyah, Dony Hidayat Al-Janan, Widya Aryadi, Ahmad Roziqin, Samsudin Anis, Wirawan Sumbodo, Jamari,

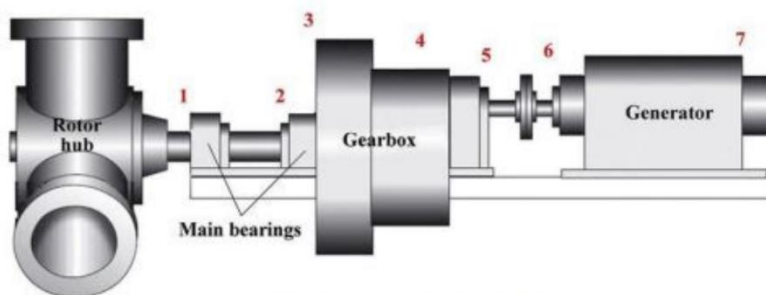Your published work in the Journal of Advanced Research in Fluid Mechanics and Thermal Sciences , volume 94, no. 1.,

Fig. 1. Main shaft bearings [10]

Analysis of an Axial Permanent Magnetic Bearing for 1MW Horizontal Axis Wind

is now available in SCOPUS database (Click here).

Kriswanto, Rizqi Fitri Naryanto, Renaldy Prasdiansyah, Dony Hidayat Al-Janan, Widya Aryadi, Ahmad Roziqin, Samsudin Anis, Wirawan Sumbodo, & Jamari. (2022). Analysis of an Axial Permanent Magnetic Bearing for 1MW Horizontal Axis Wind. Journal of Advanced Research in Fluid Mechanics and Thermal Sciences, 94(1), 172–187. https://doi.org/10.37934/arfmts.94.1.172187

Promote your works to boost your citation count. You may consider the following techniques:
• Use social media. Provide links to your papers on social media
  (e.g., Facebook, Twitter, Academia.edu, ResearchGate, Mendeley) and your university profile page.
• Talk to other researchers about your paper, and email copies of your paper to researchers who may be interested.
Create a blog or a website dedicated to your research and share it.
• Cite your own past papers as appropriate to increase visibility of your published papers.

Thank you again for publishing with us. We wish you the best success with your research.

Kind regards

"SHARE YOUR KNOWLEDGE FOR A BETTER TOMORROW"

--

SEMARAK ILMU PUBLISHING
NO. 22, Jalan Puteri 5A/3,
Bandar Puteri Bangi, 43000 Kajang,
Selangor, MALAYSIA

----

8. Publish online artikel (11 April 2022)

Analysis of an Axial Permanent Magnetic Bearing for 1MW Horizontal Axis Wind Turbine

Kriswanto[1,*], Rizqi Fitri Naryanto[1], Renaldy Prasdiansyah[1], Dony Hidayat Al-Janan[1], Widya Aryadi[1], Ahmad Roziqin[1], Samsudin Anis[1], Wirawan Sumbodo[1], Jamari[2]

[1] Department of Mechanical Engineering, Universitas Negeri Semarang, Gd E9 Kampus Sekaran Gunungpati, Semarang, Indonesia
[2] Department of Mechanical Engineering, University of Diponegoro, Jl. Prof. Sudharto Kampus UNDIP Tembalang, Semarang 50275, Indonesia

ARTICLE INFO

ABSTRACT

One way to reduce maintenance costs while improving wind turbine efficiency is to replace mechanical bearings with permanent magnetic bearings. The permanent magnetic bearing is a free contact bearing in which the rotor is elevated from the stator by the magnet's repelling force. The purpose of this study is to analyze the variation of permanent magnet width and the gap distance between the rotor-stator magnets that can produce the magnetic axial force opposing the thrust force of 1MW horizontal axis wind turbines (HAWT). The method used in this study is a magnetic force simulation using finite element method by varying the magnet thickness, width of the gap, and displacement between the rotor-stator of the PMB model. The PMB model consists of rotor and stator magnets arranged in 3 layers with Nd2Fe14B type material with a magnetic flux density of 1.45 T. Variations in thickness of the rotor and stator magnets are 0.1; 0.15, respectively; 0.2 (m), while variations in the width of the magnetic gap are 4, 5, 6 (mm). The results of the study found that the displacement that produces an axial magnetic force that can support a thrust force of 199.5kN is the lowest in the PMB model with a magnetic thickness of 0.15m with a magnetic gap of 4mm, while the highest is at a magnetic thickness of 0.1m with a magnet gap of 6mm. The greater the thickness of the PMB axial magnet design, the greater the displacement that provides zero axial magnetic forces. Further, the maximum of the magnetic axial force is rise on with increasing magnet thickness.

1. Introduction

One of the most critical components of wind turbines is the bearing. Furthermore, the wind industry has recognized main bearing failures as a major concern in terms of raising wind turbine reliability and availability, according to the European Academy of Wind Energy (EAWE) [1]. It is due to the high maintenance costs and long periods of downtime related to main bearing failures. Large-scale power plants currently apply mechanical bearings for onshore and offshore wind turbines. Nevertheless, the use of it has a limited-service life as well as capability [2]. So, the effort to improve

---